(112–408) and *in vitro* translated $^{35}$S-labeled p73α, p73β, p73α(1–548) or p53. GST alone was employed as a negative control. As shown in Figure 1c, radio-labeled p73α was pulled down by GST-RanBPM(112–408) but not by GST alone. However, p73β and p73α(1–548), which lack the extreme COOH-terminal portion of p73α, were no longer able to interact with GST-RanBPM(112–408). In addition, p53 failed to bind to GST-RanBPM(112–408). In good agreement with the yeast two-hybrid results, these observations suggest that the extreme COOH-terminal portion of p73α is responsible for the physical interaction with RanBPM. Next, we performed co-immunoprecipitation experiments to confirm their interaction in cells. To this end, cell lysates prepared from COS7 cells co-transfected with HA-tagged p73α and FLAG-tagged full-length RanBPM were immunoprecipitated with anti-p73 or anti-FLAG antibody, followed by immunoblotting with anti-FLAG or anti-HA antibody, respectively. As shown in Figure 1d, HA-p73α co-immunoprecipitated with FLAG-RanBPM. Under our experimental conditions, HA-p73α(1–427) and HA-p73α(1–247) did not co-immunoprecipitate with FLAG-RanBPM (Figure 1e). In contrast to full-length p73α, the anti-p53 immunoprecipitates did not contain FLAG-RanBPM (Figure 1f). Taken together, our results suggest that RanBPM has an ability to interact with p73α but not with p53 in mammalian cultured cells.

Previous immunostaining studies have shown that p73α is exclusively localized in cell nucleus (Jost *et al.*, 1997), while RanBPM could distribute to the cell nucleus, perinuclear region and cytoplasm (Nishitani *et al.*, 2001; Umeda *et al.*, 2003). To examine the subcellular localization of RanBPM in the presence or absence of p73α, COS7 cells were transfected with the indicated expression plasmids, and the indirect immunofluorescent staining was performed. As shown in Figure 2a and b, FLAG-RanBPM and HA-p73α were detected largely in the cytoplasm and cell nucleus, respectively. Of note, when FALG-RanBPM was co-expressed with HA-p73α, a fraction of FLAG-RanBPM translocated into cell nucleus, and co-localized with nuclear HA-p73α (Figure 2c–e). To confirm this issue, transfected COS7 cells were fractionated into nuclear and cytoplasmic fractions, and their subcellular localizations were analysed by immunoblotting. The purity of the nuclear and cytoplasmic fractions was examined by immunoblotting with anti-Lamin B and anti-α-tubulin antibody, respectively. Consistent with the indirect immunofluorescent staining, co-expression of FLAG-RanBPM with HA-p73α resulted in a significant nuclear accumulation of FLAG-RanBPM, whereas FLAG-RanBPM alone was detected in the cytoplasmic fraction (Figure 2f). In addition, the amounts of nuclear HA-p73α seemed to be increased in the presence of FLAG-RanBPM. It is thus likely that RanBPM interacts with p73α in cell nucleus, and could affect the stability of p73α.

To test whether RanBPM could affect the stability of p73α, COS7 cells were co-transfected with the constant amount of HA-p73α together with or without the

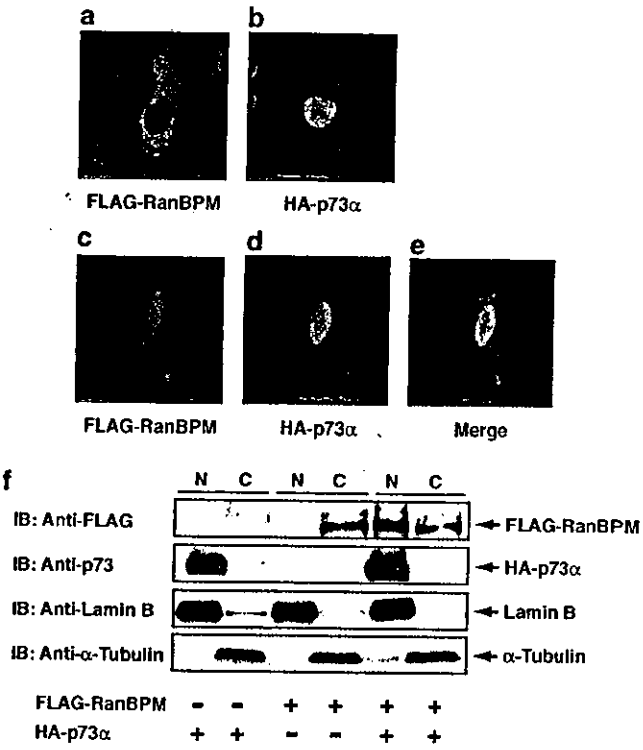


Figure 2 Subcellular distribution of RanBPM in the presence of p73. (a–e) Nuclear co-localization of p73α and RanBPM by immunofluorescence. COS7 cells were transfected with FLAG-RanBPM (a), HA-p73α (b) or FLAG-RanBPM and HA-p73α (c–e). At 48 h after transfection, cells were fixed in 20% methanol and incubated with anti-FLAG (red) and anti-HA antibody (green) (Medical and Biological Laboratories, Nagoya, Japan), followed by the incubation with the rhodamine- and FITC-conjugated secondary antibodies (Jackson ImmunoResearch Laboratories), respectively. Cells were then examined under a confocal scanning laser microscope. The merged images of the two signals are displayed in yellow (e). (f) Fractionation of COS7 cell extracts. COS7 cells were transfected with the indicated expression plasmids. At 48 h after transfection, cells were fractionated into nuclear (N) and cytoplasmic (C) fractions, and then analysed directly by immunoblotting with anti-FLAG (first panel) or anti-p73 antibody (second panel). The nuclear or cytoplasmic fraction was confirmed by immunoblotting with anti-Lamin B (Ab-1, Oncogene Research Products) (third panel) or anti-α-tubulin antibody (DM1A, Cell Signaling Technology, Beverly, MA, USA) (fourth panel), respectively

increasing amounts of FLAG-RanBPM. As shown in Figure 3a, the amount of HA-p73α was markedly increased in the presence of FLAG-RanBPM in a dose-dependent manner, whereas the expression level of p73α mRNA remained unchanged. On the other hand, FLAG-RanBPM had no significant effect on the levels of exogenous p53 (Figure 3b). Similar results were also obtained in p53-deficient H1299 cells (data not shown). We next sought to determine the half-life of p73α in the presence of RanBPM. For this purpose, COS7 cells were transfected with HA-p73α together with or without FLAG-RanBPM. At 24 h after transfection, cells were treated with cycloheximide. At the indicated time periods, cell lysates were analysed for HA-p73α by immunoblotting. In accordance with the previous reports (Lee and La Thangue, 1999; Ohtsuka *et al.*,

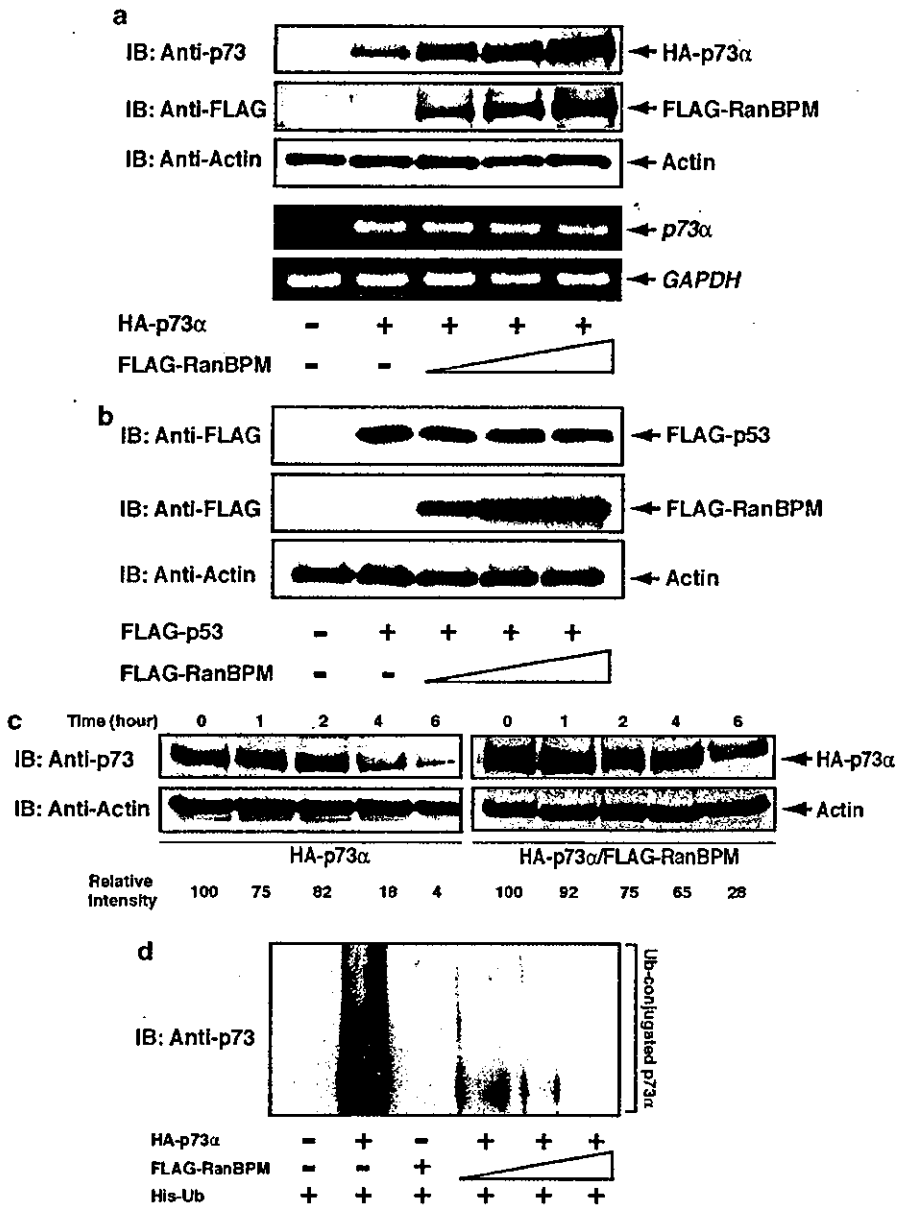


**Figure 3** RanBPM increases the stability of p73 but not of p53. (**a**) RanBPM increases the amounts of p73α. COS7 cells were co-transfected with the constant amount of HA-p73α (0.5 μg) together with or without the increasing amounts of FLAG-RanBPM (0.5, 1.0 and 1.5 μg). The total amount of plasmid DNA was kept constant (2 μg) with pcDNA3. At 48 h after transfection, cell lysates or total RNA were prepared, and subjected to immunoblotting with the indicated antibodies (upper panels) or RT–PCR analysis (lower panels). Immunoblotting for actin (20–33, Sigma Chemical Co.) serves as a loading control. (**b**) RanBPM does not affect the amounts of p53. COS7 cells were co-transfected with the indicated combinations of the expression plasmids, and were processed for immunoblotting as described above. (**c**) RanBPM increases the half-life of p73α. COS7 cells were transfected with HA-p73α alone (0.5 μg) (left panels) or together with FLAG-RanBPM (1.5 μg) (right panels). At 24 h post-transfection, cells were treated with cycloheximide (100 μg/ml) and harvested at the indicated time periods. Cell lysates were used for immunoblotting with the indicated antibodies. The intensity of the bands was quantified by using densitometry. (**d**) RanBPM inhibits the ubiquitination of p73α. COS7 cells were co-transfected with the constant amount of HA-p73α (0.5 μg) and His-tagged ubiquitin (Ub) (0.5 μg), together with or without the increasing amounts of FLAG-RanBPM (0.5, 1.0 and 1.5 μg). At 24 h post-transfection, cells were treated with 20 μM MG-132 for 6 h before being harvested. His-tagged ubiquitin-containing protein complexes were pulled down with $Ni^{2+}$-agarose beads (QIAGEN, Valencia, CA, USA), and subsequently resolved by 10% SDS-polyacrylamide gel electrophoresis, followed by immunoblotting with anti-p73 antibody

2003), ectopically expressed p73α had a half-life of less than 4 h, whereas the degradation rate of HA-p73α was slower in FLAG-RanBPM-expressing cells (Figure 3c). Thus, it is likely that the RanBPM-dependent stabilization of p73α is attributed to the clear increase in the half-life of p73α.

As described (Balint *et al*., 1999), the stability of p73 is regulated at least in part through the ubiquitin–proteasome pathway. These observations prompted us to determine whether RanBPM could prevent the ubiquitination of p73. COS7 cells were transfected with HA-p73α- and His-tagged ubiquitin, or in combination

with the increasing amounts of FLAG-RanBPM. At 24 h after transfection, cells were treated with MG-132 for 6 h. His-ubiquitinated proteins were purified by $Ni^{2+}$-agarose beads, and then analysed by immunoblotting with the anti-p73 antibody. As shown in Figure 3d, the slower migrating ubiquitinated forms of p73α were detectable in the absence of FLAG-RanBPM. Intriguingly, the ubiquitination levels of p73α were significantly reduced in cells expressing FLAG-RanBPM, suggesting that RanBPM stabilizes p73α by inhibiting its ubiquitination.

To determine whether RanBPM could affect the transcriptional activity of p73α, H1299 cells were transiently transfected with a constant amount of the expression plasmid for HA-p73α, together with the p53/p73-responsive $p21^{WAF1}$ or *MDM2* luciferase reporter constructs in the presence or absence of increasing amounts of the FLAG-RanBPM expression plasmid. As shown in Figure 4a, expression of FLAG-RanBPM enhanced the ability of p73α to transactivate the $p21^{WAF1}$ and *MDM2* promoters in a dose-dependent manner. To extend the functional significance of their interaction, we examined the possible effect of RanBPM on the p73α-mediated apoptosis. H1299 cells were transfected with HA-p73α, FLAG-RanBPM, or HA-p73α and FLAG-RanBPM. The β-galactosidase was used as a marker to visualize the transfected cells. At 48 h post transfection, the number of β-galactosidase-positive cells was scored. As shown in Figure 4b, the number of β-galactosidase-positive cells expressing FLAG-RanBPM was similar to that detected in the empty plasmid-transfected cells. Consistent with the previous report (Watanabe *et al.*, 2002), expression of HA-p73α resulted in a clear decrease in the number of β-galactosidase-positive cells. Of note, co-expression of HA-p73α with FLAG-RanBPM significantly reduced the number of β-galactosidase-positive cells as compared with that observed in cells expressing HA-p73α alone. In addition, we performed a colony formation assay. H1299 cells were transfected with HA-p73α, FLAG-RanBPM or HA-p73α plus FLAG-RanBPM, and the transfected cells were selected in the presence of G418. After 2 weeks of selection, drug-resistant colonies were fixed and stained with Giemsa's solution. In accordance with the β-galactosidase assay, FLAG-RanBPM expression did not affect the colony formation as compared with the empty plasmid-transfected control, whereas co-expression of HA-p73α with FLAG-RanBPM reduced the colony formation even more efficiently than HA-p73α alone (Figure 4c). Considering that p73α efficiently induced apoptosis in H1299 cells (Di Como *et al.*, 1999; Zeng *et al.*, 1999), these results suggest that RanBPM increases the proapoptotic activity of p73α. To further confirm this issue, H1299 cells were transiently transfected with a constant amount of the GFP expression plasmid along with the indicated combinations of the expression plasmids. At 48 h after transfection, transfected cells were identified by fluorescence microscopy for the appearance of green fluorescence, and the number of GFP-positive cells with condensed and fragmented nuclei was counted. As shown in Figure 4d, co-expression of HA-p73α with FLAG-RanBPM increased the number of apoptotic cells as compared with that resulting from expression of HA-p73α alone. Taken together, our present results strongly suggest that RanBPM-mediated stabilization of p73α is critical for its effects on transcriptional activation as well as apoptosis.

Recently, it has been shown that a variety of cellular proteins could interact with RanBPM, including MET, androgen receptor, HIPK2, USP11, Twa1, calbindin D28K and $p75^{NTR}$, suggesting that RanBPM is involved in diverse biological processes (Ideguchi *et al.*, 2002; Rao *et al.*, 2002; Wang D *et al.*, 2002; Wang Y *et al.*, 2002; Bai *et al.*, 2003; Lutz *et al.*, 2003; Umeda *et al.*, 2003). In the present study, we demonstrated that RanBPM increased the stability of p73α by reducing its ubiquitination levels. An important question raised by our results is how RanBPM stabilize p73α. Intriguingly, Ideguchi *et al.* (2002) described that RanBPM is associated with the deubiquitination enzyme USP11, which belongs to the ubiquitin hydrolase family. Considering that p53 is stabilized by direct deubiquitination by the deubiquitination enzyme HAUSP (Li *et al.*, 2002), it is likely that RanBPM could bind to USP11 and promote deubiquitination of p73α by recruiting USP11 to p73α; however, further studies will be required to determine this issue.

Alternatively, Lee and La Thangue (1999) found that p73β is much more stable than p73α, suggesting that the unique COOH-terminal portion of p73α might be critical for degradation by the ubiquitin–proteasome system. According to our present results, RanBPM bound to p73α through its extreme COOH-terminal region, whereas it failed to interact with p73β. Thus, it is plausible that RanBPM might increase the steady-state levels of p73α by masking p73α COOH-terminal lysine residues, which could be the sites for ubiquitin ligation, and/or disrupting the interaction of p73α with unknown proteins required for ubiquitination-mediated proteolysis. These possibilities are currently under investigation. Elucidation of the detailed molecular mechanism underlying the RanBPM-dependent stabilization of p73α would be necessary for better understanding of p73 turnover.

Another finding of the present study is that, under our experimental conditions, cytoplasmic RanBPM became nuclear in the presence of p73α overexpression. Given that RanBPM is localized in both the cytoplasm and nucleus (Nakamura *et al.*, 1998; Nishitani *et al.*, 2001), it is probable that p73α might have an ability to promote nuclear translocation of RanBPM through the physical interaction between them. As described previously, wild-type p53 is predominantly localized in the cytoplasm of many neuroblastoma cells (Moll *et al.*, 1996). The abnormal cytoplasmic distribution of p53 might be attributed at least in part to the interaction with Parc, which acts as a cytoplasmic anchor protein for p53 (Nikolaev *et al.*, 2003). Interestingly, Goldschneider *et al.* (2004) found that enforced expression of p73α in neuroblastoma-derived SH-SY5Y cells significantly enhances the nuclear accumulation of wild-type p53 and

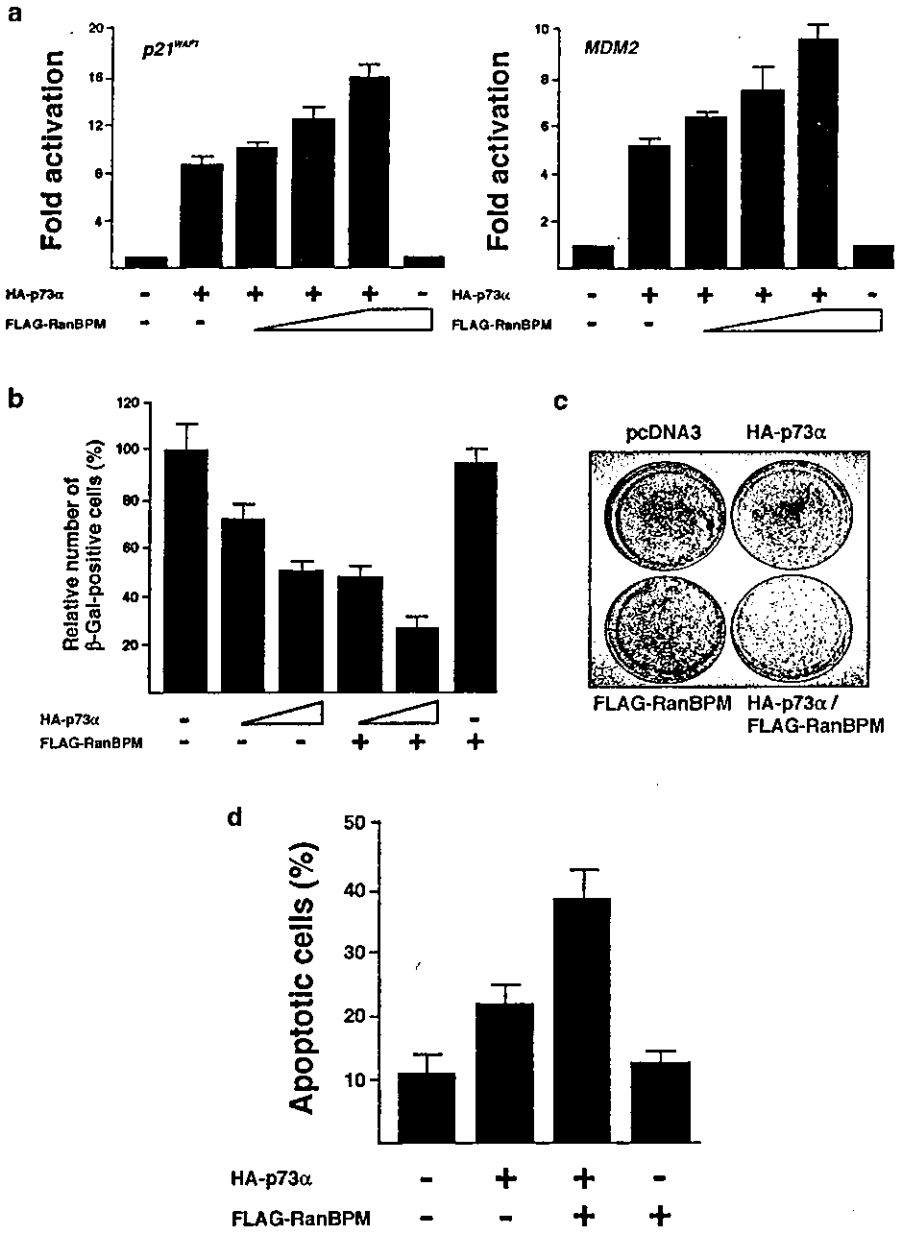


**Figure 4** RanBPM enhances p73 function. (**a**) RanBPM enhances the transcriptional activity of p73α. p53-deficient H1299 cells were co-transfected with 25 ng of the expression plasmid for HA-p73α together with 100 ng of p53/p73-responsive *p21*$^{WAF1}$ (left panel) or *MDM2* (right panel) luciferase reporter construct, and 10 ng of the *Renilla* luciferase plasmid (pRL-TK, Promega Corp., Madison, WI, USA), in the presence or absence of increasing amounts of the FLAG-RanBPM expression plasmid (25, 50, or 100 ng). At 48 h after transfection, cells were lysed and their luciferase activities were measured. Firefly luminescence signal was normalized based on the *Renilla* luminescence signal. (**b**) RanBPM stimulates the p73α-mediated growth suppression. H1299 cells were co-transfected with the indicated combinations of the expression plasmid together with the constant amount of the expression plasmid for β-galactosidase (125 ng) (pCH110, Amersham Pharmacia Biotech). At 48 h after transfection, transfected cells were identified by staining with 5-bromo-4-chloro-3-indolyl-β-D-galactopyranoside (X-gal). The relative percentage of β-gal-positive cells represents the ratio of the number of β-gal-positive cells to that of those transfected with pcDNA3 alone. (**c**) Colony formation assay. H1299 cells were transfected with HA-p73α (200 ng), FLAG-RanBPM (750 ng) or HA-p73α (200 ng) plus FLAG-RanBPM (750 ng). Total amount of plasmid DNA was kept constant (1 μg) with pcDNA3, and pcDNA3 alone was used as a negative control. At 2 days after transfection, cells were selected with G418 (400 μg/ml) for 2 weeks. G418-resistant colonies were fixed in methanol, and stained with Giemsa's solution. Representative dishes of three independent experiments are shown. (**d**) RanBPM enhances the p73α-mediated apoptosis. H1299 cells transfected with 0.2 μg of the GFP expression plasmid and 0.5 μg of the HA-p73α expression plasmid together with or without 1.5 μg of the FLAG-RanBPM expression plasmid. At 48 h after transfection, transfected cells were identified by the presence of green fluorescence. Cell nucleus was stained with DAPI to reveal nuclear condensation and fragmentation. The number of GFP-positive cells with apoptotic nuclei was scored

restores its function, indicating that p73α displaces p53 from the cytoplasmic complex containing Parc. It is thus likely that p73α could modulate cellular proteins/pathways that specifically regulate nuclear import and export of RanBPM. Since RanBPM is associated with a variety of nuclear proteins, p73α might play a critical role in regulating nuclear function of RanBPM.

**Acknowledgements**
We are grateful to Dr S Sakiyama for helpful discussion. This work was supported in part by a Grant-in-Aid from the Ministry of Health and Welfare for a New 10-Year Strategy for Cancer Control, a Grant-in-Aid for Scientific Research on Priority Areas, a Grant-in-Aid for Scientific Research (B) from the Ministry of Education, Science, Sports and Culture, Japan, and a found from the Hisamitsu Pharmaceutical Company.

**References**

Agami R, Blandino G, Oren M and Shaul Y. (1999). *Nature*, **399**, 809–813.
Bai D, Chen H and Huang BR. (2003). *Biochem. Biophys. Res. Commun.*, **309**, 552–557.
Balint E, Bates S and Vousden KH. (1999). *Oncogene*, **18**, 3923–3929.
Carrano AC, Eytan E, Hershko A and Pagano M. (1999). *Nat. Cell Biol.*, **1**, 193–199.
Di Como CJ, Gaiddon C and Prives C. (1999). *Mol. Cell. Biol.*, **19**, 1438–1449.
Ganoth D, Bornstein G, Ko TK, Larsen B, Tyers M, Pagano M and Hershko A. (2001). *Nat. Cell Biol.*, **3**, 321–324.
Goldschneider D, Blanc E, Raguenez G, Barrois M, Legrand A, Le Roux G, Haddada H, Bebard J and Douc-Rasy S. (2004). *J. Cell Sci.*, **117**, 293–301.
Gong J, Costanzo A, Yang H-Q, Melino G, Kaelin WG, Levrero M and Wang JYJ. (1999). *Nature*, **399**, 806–809.
Ideguchi H, Ueda A, Tanaka M, Yang J, Tsuji T, Ohno S, Hagiwara E, Aoki A and Ishigatsubo Y. (2002). *Biochem. J.*, **367**, 87–95.
Jost C, Marin M and Kaelin WG. (1997). *Nature*, **389**, 191–194.
Kaghad M, Bonnet H, Yang A, Creancier L, Biscan JC, Valent A, Minty A, Chalon P, Lelias JM, Dumont X, Ferrara P, McKeon F and Caput D. (1997). *Cell*, **90**, 809–819.
Lee C-W and La Thangue NB. (1999). *Cncogene*, **18**, 4171–4181.
Li M, Chen D, Shiloh A, Luo J, Nikolaev AY, Qin J and Gu W. (2002). *Nature*, **416**, 648–653.
Lutz W, Frank EM, Craig TA, Thompson R, Venters RA, Kojetin D, Cavanagh J and Kumar R. (2003). *Biochem. Biophys. Res. Commun.*, **303**, 1186–1192.
Melino G, De Laurenzi V and Vousden KH. (2002). *Nat. Rev. Cancer*, **2**, 605–615.
Moll UM, Ostermeyer AG, Haladay R, Winkfield B, Frazier M and Zambetti G. (1996). *Mol. Cell. Biol.*, **16**, 1126–1137.
Nakagawa T, Takahashi M, Ozaki T, Watanabe K, Todo S, Mizuguchi H, Hayakawa T and Nakagawara A. (2002). *Mol. Cell. Biol.*, **22**, 2575–2585.
Nakamura M, Masuda H, Horii J, Kuma K, Yokoyama N, Ohba T, Nishitani H, Miyata T, Tanaka M and Nishimoto T. (1998). *J. Cell Biol.*, **143**, 1041–1052.
Nikolaev AY, Li M, Puskas N, Qin J and Gu W. (2003). *Cell*, **112**, 29–40.
Nishitani H, Hirose E, Uchimura Y, Nakamura N, Umeda M, Nishii K, Mori N and Nishimoto T. (2001). *Gene*, **272**, 25–33.
Ohtsuka T, Ryu H, Minamishima YA, Ryo A and Lee SW. (2003). *Oncogene*, **22**, 1678–1687.
Ozaki T, Watanabe K, Nakagawa T, Miyazaki K, Takahashi M and Nakagawara A. (2003). *Oncogene*, **22**, 3231–3242.
Ponting C, Schultz J and Bork P. (1997). *Trends Biochem. Sci.*, **22**, 193–194.
Pozniak CD, Radinovic S, Yang A, McKeon F, Kaplan DR and Miller FD. (2000). *Science*, **289**, 304–306.
Rao MA, Cheng H, Quayle AN, Nishitani H, Nelson CC and Rennie PS. (2002). *J. Biol. Chem.*, **277**, 48020–48027.
Ren J, Datta R, Shioya H, Li Y, Oki E, Biedermann V, Bharti A and Kufe D. (2002). *J. Biol. Chem.*, **277**, 33758–33765.
Stiewe T, Zimmermann S, Frilling A, Esche H and Putzer BM. (2002). *Cancer Res.*, **62**, 3598–3602.
Umeda M, Nishitani H and Nishimoto T. (2003). *Gene*, **303**, 47–54.
Wang D, Li Z, Messing EM and Wu G. (2002). *J. Biol. Chem.*, **277**, 36216–36222.
Wang Y, Schneider M, Li X, Duttenhofer I, Debatin K-M and Hug H. (2002). *Biochem. Biophys. Res. Commun.*, **297**, 148–153.
Watanabe K, Ozaki T, Nakagawa T, Miyazaki K, Takahashi M, Hosoda M, Hayashi S, Todo S and Nakagawara A. (2002). *J. Biol. Chem.*, **277**, 15113–15123.
Yuan Z-M, Shioya H, Ishiko T, Sun X, Gu J, Huang YY, Lu H, Kharbanda S, Weichselbaum R and Kufe D. (1999). *Nature*, **399**, 814–817.
Zeng X, Chen L, Jost CA, Maya R, Keller D, Wang X, Kaelin WG, Oren M, Chen J and Lu H. (1999). *Mol. Cell. Biol.*, **19**, 3257–3266.

Oncogene (2003) 22, 5525–5536

www.nature.com/onc

# Expression profiling and characterization of 4200 genes cloned from primary neuroblastomas: identification of 305 genes differentially expressed between favorable and unfavorable subsets

Miki Ohira[1], Aiko Morohashi[1], Hiroyuki Inuzuka[1], Tomotane Shishikura[1], Takemasa Kawamoto[1], Hajime Kageyama[1], Yohko Nakamura[1], Eriko Isogai[1], Hajime Takayasu[1], Shigeru Sakiyama[1], Yutaka Suzuki[2], Sumio Sugano[2], Takeshi Goto[3], Shuji Sato[3] and Akira Nakagawara*,[1]

[1]*Division of Biochemistry, Chiba Cancer Center Research Institute, 666-2 Nitona, Chiba 260-8717, Japan;* [2]*Department of Cancer Virology, Institute of Medical Science, University of Tokyo, Tokyo 108-8639, Japan;* [3]*Hisamitsu Co., Inc., 1-11-1 Marunouchi, Chiyoda-ku, Tokyo 100-622, Japan*

**Neuroblastoma (NBL), one of the most common childhood solid tumors, has a distinct nature in different prognostic subgroups: NBL in patients under 1 year of age usually regresses spontaneously, whereas that in patients over 1 year of age often grows aggressively and eventually kills the patient. To understand the molecular mechanism of biology and tumorigenesis of NBL, we decided to perform a comprehensive approach to unveil the gene expression profiles among the NBL subsets. We constructed the subset-specific oligo-capping cDNA libraries from the primary NBL tissues with favorable (F: stage 1, high expression of *TrkA* and a single copy of *MYCN*) and unfavorable (UF: stage 3 or 4, decreased expression of *TrkA* and *MYCN* amplification) characteristics and randomly cloned 4654 cDNAs. Among 4243 cDNAs sequenced successfully, 1799 (42.4%) were the genes with unknown function. Excluding the housekeeping genes, an expression profile of each subset was extremely different. To determine the genes expressed differentially between F and UF subsets, we performed semiquantitative reverse transcriptase (RT)–PCR for each of the 1842 independent genes using RNA obtained from 16 F and 16 UF NBLs as template. This revealed that 278 genes were highly expressed in the F subset as compared to the UF one, while, surprisingly, only 27 genes were expressed at higher levels in the UF rather than the F subset. These differentially expressed genes included 194 genes with unknown function. Many of the genes expressed at high levels in the F subset were related to catecholamine biosynthesis, small GTPases, synapse formation, synaptic vesicle transport, and transcription factors regulating differentiation of the neural crest-derived cells. On the other hand, the genes expressed at high levels in the UF subset included transcription factors and/or receptors that might regulate neuronal growth and differentiation. The chromosomal mapping of those genes showed some clusters. Thus, our mass-identification and characterization of the differentially expressed genes between the subsets may become a powerful tool for finding the important genes of NBL as well as developing new diagnostic and therapeutic strategies against aggressive NBL.**

*Oncogene* (2003) **22**, 5525–5536. doi:10.1038/sj.onc.1206853

**Keywords:** neuroblastoma; expression profile; oligo-capping cDNA library; differentiation; regression; MYCN

## Introduction

Neuroblastoma (NBL) is a pediatric cancer originating from sympathoadrenal lineage of the neural crest. However, its clinical behavior is enigmatic. It often regresses spontaneously when the tumor occurs in patients less than 1 year of age, while it is usually aggressive when it occurs in those over 1 year of age (Brodeur and Nakagawara, 1992). Accumulating evidence suggests that the NBL regression is at least in part regulated by developmentally programmed neuronal cell death (PNCD) and/or neuronal differentiation that are similar to the phenomena occurring in normal sympathetic neurons during their development. In contrast, aggressive NBLs continue to grow with enhanced invasiveness and metastasis to the specific regions such as bones and distant lymph nodes.

The recent advances in NBL research have revealed cytogenetic as well as molecular biological bases of this tumor. NBLs in advanced stages often possess a frequent loss of the distal part of the short arm of chromosome 1 (1p), amplification of the *MYCN* oncogene and gain of chromosome 17q (Brodeur *et al.*, 1984; Caron *et al.*, 1995). These genetic aberrations are also good prognostic markers. On the other hand, the recent studies have revealed that the biology of NBL is strongly regulated by neurotrophins and their receptors,

*Correspondence: A Nakagawara;
E-mail: akiranak@chiba-ccri.chuo.chiba.jp
Received 25 November 2002; revised 23 April 2003; accepted 9 June 2003

which is similar to the control of growth, differentiation and programmed cell death in the neural crest-derived cells during the development (Anderson and Axel, 1985; Nakagawara, 1998). TRK-A, a high-affinity receptor for nerve growth factor (NGF), has been shown to be expressed in NBLs with favorable prognosis and probably regulate the differentiation and/or regression of the tumor (Nakagawara *et al.*, 1993). In contrast, *TRK-B*, encoding a receptor for brain-derived neurotrophic factor and neurotrophin-4/5, is frequently expressed in the tumors with *MYCN* amplification, which promotes cell survival and increases the invasive ability (Nakagawara *et al.*, 1994; Matsumoto *et al.*, 1995). Moreover, signaling from the GDNF family and their receptors, Ret and GFRα, appear to play an important role in regulating differentiation of NBL cells (Hishiki *et al.*, 1998). The other neurotrophic factors, pleiotrophin (PTN) and midkine (MK), are also differentially expressed in different subsets of primary NBL (Nakagawara *et al.*, 1995). However, those cytogenetic and biological markers are still not always enough to predict the prognosis in certain populations of NBL patients.

To understand the molecular mechanism of genesis and biology of NBL as well as to develop novel diagnostic and therapeutic tools, we have cloned a large number of genes expressed in each subset of primary NBL by using full-length-enriched oligo-capping cDNA libraries. In the present study, we have identified more than 300 genes that are differentially expressed between F and UF subsets, most of which were preferentially expressed in favorable NBLs.

## Results

### *Construction of oligo-capping neuroblastoma cDNA libraries and DNA sequencing*

Figure 1 shows the scheme of our neuroblastoma cDNA project. The oligo-capping cDNA libraries were constructed from three anonymous primary NBL tissues with favorable characteristics (F: stage 1, high expression of *TrkA* and a single copy of *MYCN*) and three NBL tissues with unfavorable biology (UF: stage 3 or 4, low expression of *TrkA* and amplification of *MYCN*). Three cDNA library solutions in each group were mixed before randomly picking up 2500 clones from each mixture. Single-run sequencing from both ends of the gene and homology search against the public databases by BLAST program was then performed. We finished sequencing of 2410 clones from the F-NBL library and 2244 clones from the UF-NBL library. The average insert size in both libraries was approximately 2.5 kb. About 53 and 56% of clones were identical to known genes in the F and the UF libraries, respectively. The rest appeared to be novel genes with unknown functions, which included those only hitting to human expressed sequence tags (ESTs), high throughput genome sequences (htgs) and nothing (Genbank release 122, Jan. 2001; Table 1).

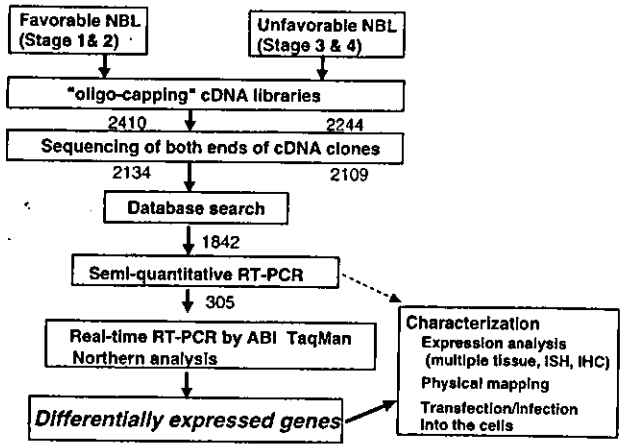


Figure 1 Scheme for the strategy of the neuroblastoma cDNA project. ISH, *in situ* hybridization, IHC, immunohistochemistry

### *Expression profile of the known genes in favorable and unfavorable neuroblastomas*

Table 2 shows the expression profile of the known genes in F and UF NBL libraries. When the housekeeping genes such as *polypeptide chain elongation factor, protein synthesis initiation factor* and *ribosomal proteins* were excluded, the nervous system-specific genes were frequently listed up. They included a kinase regulator, *14-3-3 epsilon*, playing a role in neural development (McConnell *et al.*, 1995), *P311* abundantly expressed in neuronal cells (Studler *et al.*, 1993), *SCG10* encoding a neuronal growth-associated protein (Anderson and Axel, 1985) and *N-cadherin*, a calcium-dependent cell–cell adhesion glycoprotein (Hirano *et al.*, 1987). The gene frequently hit among these neuronal genes was *14-3-3 epsilon* (9 times in the F library and 7 times in the UF library). Clustering analysis using BLAST homology search program found 1844 of gene groups and 1669 of these were in the F and the UF libraries, respectively. Of these, only 110 gene groups were overlapped between the two libraries, suggesting that the expression profile was markedly different between both libraries. In the UF library, the genes related to protein synthesis like *polypeptide chain elongation factor* and *protein synthesis initiation factor* were much more frequent as compared to those in the F library (Table 2). Notable was a frequency of the DEAD box motif gene*DDX1* (69 clones in the UF library) that appeared only once in the F library. As the *DDX1* gene was closely linked to and coamplified with the *MYCN* gene (Amler *et al.*, 1996; Noguchi *et al.*, 1996), this expression pattern also reflects the nature of the origins of libraries. However, our preliminary study suggested that the difference of the hit numbers of the genes did not necessarily reflect their differential expression between both subsets.

### *Identification of the genes differentially expressed between favorable and unfavorable neuroblastomas*

To identify the genes expressed differentially between the F and UF subsets, all independent clones except the

Table 1 Results of homology search by BLASTN

| | *Number of clones obtained from the cDNA library* | | | |
|---|---|---|---|---|
| | *Favorable NBL* | | *Unfavorable NBL* | |
| Human known genes | 1060 | 1129 (52.9%) | 1175 | 1184 (56.1%) |
| Known genes of other species | 69 | | 9 | |
| ESTs | 477 | 880 (41.2%) | 436 | 919 (43.6%) |
| Human genome sequences | 307 | | 285 | |
| No hit | 96 | | 198 | |
| Repeats (SINEs, LINEs) | 125 | | 6 | |
| Total | 2134 (2410 sequenced) | | 2109 (2244 sequenced) | |

housekeeping genes from both libraries were subjected to semiquantitative RT–PCR analysis. The complementary DNA reverse-transcribed from total RNA obtained from 16 F and 16 UF primary NBLs was used as the PCR template after normalization with *GAPDH* (and also with *β-actin*) expression (Figure 2, see Materials and methods). In total, 1842 independent genes including 1152 unknown genes and 690 known genes from both libraries were surveyed. As a result, we found that at least 305 (16.6%) genes displayed a distinct pattern of differential expression (Table 3). Among the 305 genes, 278 (109 known and 169 unknown genes) were expressed at higher levels in F than UF NBLs. On the other hand, only 27 genes (two known and 25 unknown genes) were found to be expressed at higher levels in UF than F NBLs (Table 3). This RT–PCR screening was repeated at least twice with each gene-specific primer set. Figure 2 shows the representatives of the results of differential screening by semiquantitative RT–PCR. The expression patterns of *DDX-1*, *TrkA*, *TrkB* and *MYCN* as controls were similar to the previous reports, indicating that our differential screening system using RT–PCR was reliable.

### *Categorization of the differentially expressed genes*

The NBL subset-related genes may include those regulating neuronal growth, differentiation and apoptosis as well as those concerning generation and progression of NBL. We classified the differentially expressed genes into nine categories according to their known functions as shown in Table 4. The genes preferentially expressed in the F-subset showed an interesting profile as follows. (a) Signaling molecules: This group included certain protein kinases and protein phosphatases, among which protein kinase C zeta (PKCzeta) showed the most distinct F-subset-specific expression pattern. A small GTPase, RAB6B and a GTP-binding protein, RAB3C, functioning in the synaptic vesicles were also found in this group. Three members of dihydropyrimidinase-related genes (DRP-1, -2, -3), which might be involved in axonal outgrowth and pathfinding as a collapsin response mediator (Hamajima *et al.*, 1996), were also included. Among these family members, DRP-2 showed the most typical F-subset-specific expression. Furthermore, the genes with neural function, like SCG10, stathmin-like-protein RB', neurexophilin, LIS1 and doublecortin were involved. SCG10 was first shown to be the gene induced in neural crest cells when they differentiate into sympathetic neurons and is also known to be a membrane-associated, microtubule-destabilizing protein of neuronal growth cones. Stathmin-like splicing variant RB' gene is a family member of SCG10 and may have a similar function. It showed more distinct difference in its expression pattern than SCG10. (b) Cell cycle-related genes, PRC1 (required for cytokinesis) and tyrosine phosphatase CDC25B (required for entry into mitosis, interacting with 14-3-3 proteins), were included. (c) Cytoskeleton and adhesion molecules: There were some members of the cadherin superfamily like protocadherins alpha 9, beta 12 and gamma A8 (neural cell–cell interaction), laminine alpha4 (neurite outgrowth), peripherin (a type III intermediate filament protein in the mammalian peripheral nervous system) and fibronectin receptor beta subunit (cell–cell connection). Among these transcripts, the most distinct pattern of differential expression was shown by peripherin. (d) Transcriptional regulators: This group included homeodomain-containing transcription factors SHOX2 (short stature homeobox homolog of Drosophila, a member of paired-related family), CUTL1 (Drosophila homeoprotein cut homolog), ZHX1 (zinc-fingers and homeodomain transcription factor 1), chromatin-modifying molecules CHD2 and CHD4 (chromodomain helicase DNA-binding proteins), PHF1 (polycomb-like), MOZ (Monocytic leukemia zinc-finger protein, a putative acetyltransferase), BAZ2B (containing a bromodomain and a PHD-finger) and HIRIP3 (related to chromatin assembly). (e) Protein synthesis, transport and turn over: There were EXO70 and SEC5, Exocyst component proteins 70 and 107 kDa, specifically located at the sites of vesicle fusion (required for exocytosis), proton-coupled divalent metal ion transporters SLC11A3 and SLC25A13, and UbcH7 and Rsp5 (related to ubiquitin–proteasome protein degradation system) in this group. (f) Metabolic enzymes, homeostasis: Drosophila shaker-related potassium voltage-gated channels KCNAB1 and KCNAB2 were found in this category. Catecholamine-related genes, dopamine β-hydroxylase type a (DBH) and monoamine oxidase type A (MAO) displayed a distinct differential expression pattern. The neurotransmitter synthesis-related genes, such as neuronal nicotinic acetylcholine receptor α-7 subunit and β-adrenergic

**Table 2** Known genes that frequently appeared in the neuroblastoma cDNA libraries

| *Accession no.* | *Definition* | *No. of clones that appeared in F library (2134)* | *No. of clones that appeared in UF library (2109)* | *Total no. (4243)* |
|---|---|---|---|---|
| E02628 | cDNA coding for human polypeptide chain elongation factor-1 alpha. | 30 | 188 | 218 |
| X70649 | HSCL1042 Homo sapiens DDX1 gene, complete CDS. | 1 | 69 | 70 |
| K00558 | HUMTUBAK human alpha-tubulin mRNA, complete cds. | 9 | 24 | 33 |
| G27412 | gb\|AF083243\|HSPC025 Homo sapiens HSPC025 mRNA, complete cds. | 11 | 20 | 31 |
| M16660 | HUMHSP90 Human 90 kDa heat-shock protein gene, cDNA, complete cds | 6 | 22 | 28 |
| S79942 | S79942 EIF4A2 = protein synthesis initiation factor 4A-II homolog [human, fetal lung tissue, mRNA Partial, 1881 nt]. | 9 | 17 | 26 |
| Z23064 | H.sapiens mRNA gene for hnRNP G protein. | 3 | 18 | 21 |
| X63432 | H. sapiens ACTB mRNA for mutant beta-actin (beta'-actin). | 17 | 2 | 19 |
| X73685 | CAHSP *C.aethiops* hsp 70 mRNA. | 14 | 4 | 18 |
| U20972 | HSU20972 Human 14-3-3 protein epsilon isoform mRNA, complete cds. | 9 | 7 | 16 |
| U88968 | HSU88968 Human alpha enolase like 1 (ENO1L1) mRNA, partial cds. | 1 | 12 | 13 |
| S72008 | S72008 hCDC10 = CDC10 homolog [human, fetal lung; mRNA, 2314 nt]. | 2 | 9 | 11 |
| X59066 | HSATPF 1M Human mRNA for mitochondrial ATP synthase (F1-ATPase) alpha subunit. | 2 | 9 | 11 |
| AF053070 | AF053070 Homo sapiens NADH:ubiquinone dehydrogenase 51 kDa subunit (NDUFV1) mRNA, nuclear gene encoding mitochondrial protein, complete cds. | 3 | 8 | 11 |
| AF070600 | AF070600 Homo sapiens clone 24464 beta-tubulin mRNA, complete cds. | 3 | 8 | 11 |
| U30521 | HSU30521 Human p311 HUM (3.1) mRNA, complete cds. | 5 | 6 | 11 |
| U46025 | HSU46025 Human translation initiation factor eIF-3 p110 subunit gene, complete cds. | 7 | 4 | 11 |
| X06747 | Human hnRNP core protein A1. | 3 | 7 | 10 |
| Y13286 | HSY13286 Homo sapiens mRNA for GDP dissociation inhibitor beta. | 4 | 6 | 10 |
| E12458 | E12458 cDNA encoding human polyubiquitin. | 8 | 2 | 10 |
| X63526 | HSEF1G H. sapiens mRNA for protein homologous to elongation factor 1-gamma from *A.salina*. | 1 | 8 | 9 |
| L22009 | HUM49KDA Human hnRNP H mRNA, complete cds. | 5 | 4 | 9 |
| X02152 | HSLDHAR Human mRNA for lactate dehydrogenase-A (LDH-A, EC1.1.1.27). | 0 | 8 | 8 |
| D23660 | HUMRSP Human mRNA for ribosomal protein, complete cds. | 5 | 3 | 8 |
| S38729 | S38729 Ku autoantigen p70 subunit [human, mRNA, 2123 nt]. | 2 | 5 | 7 |
| M86667 | HUMNAP H. sapiens NAP (nucleosome assembly protein) mRNA, complete cds. | 4 | 3 | 7 |
| X59798 | HSPRAD1CY Human PRAD1 mRNA for cyclin. | 4 | 3 | 7 |
| M60858 | HUMNUCLEO Human nucleolin gene, complete cds. | 1 | 5 | 6 |
| M29877 | HUMALFUC Human alpha-L-fucosidase, complete cds. | 3 | 3 | 6 |
| A31920 | A31920 H. sapiens calmodulin gene. | 3 | 3 | 6 |
| U32996 | HSMAP19 Human microtubule-associated protein -2 (MAP 2) gene, exon 19. | 3 | 3 | 6 |
| AB008109 | Homo sapiens mRNA for RGS5, complete cds. | 5 | 1 | 6 |
| AF026292 | AF026292 Homo sapiens chaperonin containing t-complex polypeptide 1, eta subunit (Ccth) mRNA, complete cds. | 0 | 5 | 5 |
| L11932 | HUMSHMTB Human nuclear-encoded mitochondrial serine hydroxymethyltransferase (SHMT) mRNA, 3'end. | 0 | 5 | 5 |

| | | | | |
|---|---|---|---|---|
| AF046001 | AF046001 Homo sapiens zinc-finger transcription factor (ZNF207) mRNA, complete cds. | 1 | 4 | 5 |
| X74801 | H. sapiens Cctg mRNA for chaperonin. | 2 | 3 | 5 |
| D13748 | Human mRNA for eucaryotic initiation factor 4AI. | 2 | 3 | 5 |
| L25899 | HUMRP10A Human ribosomal protein L10 mRNA, complete cds. | 2 | 3 | 5 |
| D31885 | HUMORFKG1N Human mRNA for KIAA0069 gene, partial cds. | 2 | 3 | 5 |
| AF000364 | Homo sapiens heterogeneous nuclear ribonucleoprotein R mRNA, complete cds. | 3 | 2 | 5 |
| D78013 | Homo sapiens mRNA for dihydropyrimidinase-related protein-2, complete cds. | 3 | 2 | 5 |
| U68105 | HSPABPS 13 Human poly(A)-binding protein(PABP) gene, exon 15. | 3 | 2 | 5 |
| AC004999 | gi\|1705541\|sp\|P19022\|CAD2_HUMAN NEURAL-CADHERIN PRECURSOR (*N*-CADHERIN)(CADHERIN-2) Length = 906 | 3 | 2 | 5 |
| L27631 | HUMAPLP2A Human amyloid precursor-like protein 2 (APLP2) mRNA, complete cds. | 4 | 1 | 5 |
| S82024 | S82024 SCG10 = neuron-specific growth-associated protein/stathmin homolog [human, embryo, mRNA, 696 nt]. | 4 | 0 | 4 |
| AJ007398 | HSA7398 Homo sapiens mRNA for PBK1 protein. | 0 | 4 | 4 |
| U31814 | HSU31814 Human transcriptional regulator homolog RPD3 mRNA, complete cds. | 0 | 4 | 4 |
| D13627 | HUMRSC548 Human mRNA for KIAA0002 gene, complete cds. | 0 | 4 | 4 |
| D14812 | HUMORF16 Human mRNA for KIAA0026 gene, complete cds. | 0 | 4 | 4 |
| AF026291 | AF026291 Homo sapiens chaperonin containing t-complex polypeptide 1, delta subunit (Cctd) mRNA, complete cds. | 0 | 4 | 4 |
| X76013 | HSGLTSY H. sapiens QRSHs mRNA for glutaminyl-tRNA synthetase. | 1 | 3 | 4 |
| X98248 | HSGP95SOR H. sapiens mRNA for sortilin, | 1 | 3 | 4 |
| D78014 | D78014 Homo sapiens mRNA for dihydropyrimidinase-related protein-3, complete cds. | 2 | 2 | 4 |
| AB007868 | Homo sapiens KIAA0408 mRNA, complete cds. | 4 | 0 | 4 |
| NM_006373 | Homo sapiens membrane protein of cholinergic synaptic vesicles. | 4 | 0 | 4 |
| U50733 | HSU50733 Human dynamitin mRNA, complete cds. | 0 | 3 | 3 |
| X97548 | HSZFPKR H. sapiens mRNA for TIF 1 beta zinc-finger protein. | 0 | 3 | 3 |
| D43950 | HUMKG1DD Human mRNA for KIAA0098 gene, partial cds. | 0 | 3 | 3 |
| AB002330 | AB002330 Human mRNA for KIAA0332 gene, partial cds. | 0 | 3 | 3 |
| AF026293 | AF026293 Homo sapiens chaperonin containing t-complex polypeptide 1, beta subunit (Cctb) mRNA, complete cds. | 1 | 2 | 3 |
| AJ000519 | HSUBICONJ Homo sapiens mRNA for ubiquitin-conjugating enzyme UbcH7. | 3 | 0 | 3 |
| L13385 | Homo sapiens (clone 71) Miller–Dieker lissencephaly protein (LIS1) mRNA, complete cds. | 3 | 0 | 3 |
| L19760 | HUMSNAP25A Human nerve-terminal protein (isoform SNAP25A) mRNA, complete cds. | 3 | 0 | 3 |
| U27768 | HSU27768 Human RGP4 mRNA, complete cds. | 3 | 0 | 3 |
| U47742 | HSU47742 Human manocytic leukemia zinc-finger protein (MOZ) mRNA, complete cds. | 3 | 0 | 3 |
| U54558 | HSU54558 Human translation initiation factor eIF3 p66 subunit mRNA, complete cds. | 3 | 0 | 3 |
| D43951 | HUMKG1EE Human mRNA for KIAA0099 gene, complete cds. | 3 | 0 | 3 |
| D63475 | D63475 Human mRNA for KIAA009 gene, complete cds. | 3 | 0 | 3 |
| AB007896 | Homo sapiens KIAA0436 mRNA, partial cds. | 3 | 0 | 3 |
| AB018347 | AB018347 Homo sapiens mRNA for KIAA0804 protein, partial cds. | 3 | 0 | 3 |
| M23725 | HUMPKM2L Human M2-type pyruvate kinase, complete cds. | 3 | 0 | 3 |

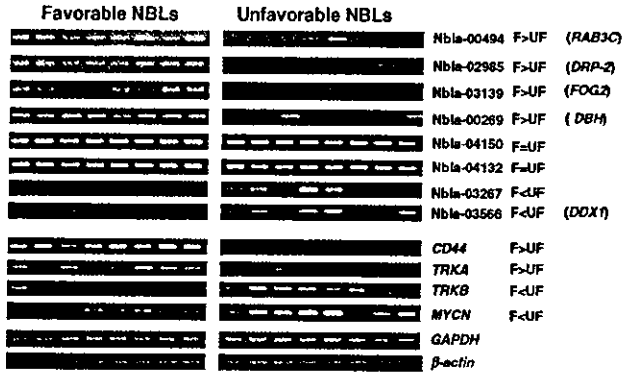


**Figure 2** Semiquantitative RT–PCR for the genes obtained from cDNA libraries of favorable and unfavorable subsets of neuroblastoma. cDNA was synthesized from 16 RNA samples of each subset and was used as a PCR template. All 16 tumors with the favorable prognosis were in stage 1, no *MYCN* amplification and a high expression of *TRKA*, while the 16 tumors with the unfavorable prognosis were in stage 3 or 4, exhibiting high *MYCN* amplification and low *TrkA* expression. In this figure, the results of the eight samples from each subset are shown. F, favorable, UF, unfavorable

**Table 3** Differentially expressed genes in neuroblastoma libraries

| | *F library* | | *UF library* | | |
|---|---|---|---|---|---|
| | *Unknown* | *Known* | *Unknown* | *Known* | *Total* |
| F>UF | 87 | 63 | 82 | 46 | 278 |
| F≒UF | 684 | 234 | 274 | 345 | 1537 |
| F<UF | 17 | 1 | 8 | 1 | 27 |
| Total | 788 | 298 | 364 | 392 | 1842 |

receptor kinase 2 were also found. These differentially expressed genes may reflect the biological status of a favorable subset of NBL which is undergoing neuronal cell growth, migration and differentiation. Interestingly, we also found hematopoiesis-related or leukemia-related genes, like MLLT4 (Trithorax homolog), MTG8-like protein, MOZ and GATA-binding protein FOG2 as differentially expressed genes.

As for the UF-subset-specific (F<UF) genes, only two were reported genes. *DDX1* had been already reported to be coamplified with *MYCN* gene in UF neuroblastomas. h*NLRR-1* was a human homolog of mouse *neuronal leucine-rich repeat protein-1* gene whose molecular function has not been clear (Taguchi *et al.*, 1996). This is the first report of h*NLRR-1* as a predominantly expressed gene in unfavorable NBLs. We have also found a new family member of *hNLRR* in our cDNA libraries, which shows an expression pattern opposite to that of *hNLRR-1* (Hamano *et al.*, under preparation). Like Trk family receptors, hNLRR family receptors may play an important role in regulating NBL biology.

### *Chromosomal mapping of the differentially expressed genes in NBL*

To examine the correlation between the differential expression in NBLs and chromosomal rearrangement or epigenetic regulatory loci, we searched for the physical location of the differentially expressed genes by BLAT search of the UC Santa Cruz genome database (http://genome.ucsc. edu/goldenPath/hgTracks.html). Among 305 candidate genes with the differential expression, 299 independent genes were able to be mapped on chromosomal bands (Figure 3). Although we expected that the majority of the differentially expressed genes might be mapped on the regions already known to be the loci with loss of heterozygosity (LOH) or amplification, the results were diverse. More than 10% of the genes were mapped on chromosomes 2 (38 genes) and 7 (35 genes). There were some clusters of genes (F>UF) at the loci of 2q31.1, 5q11.2, 6p22.3, 6q21, 7p15.1, 7q21.11, 7q21.3, 7q31.1, 9q34.2, 11q13.4, 13q13.3, 15q21.1 and 22q12.2, among which the regions of 2q31.1, 5q11.2 and 9q34.2 were notable. The chromosome 9q34–qter region has been reported to display a high frequency of LOH by Takita *et al.* (1997), whereas the former two regions so far have no evidence of high frequency of LOH. On chromosome 9q34.2, three known (one of them was *DBH*) and one novel gene with high expression in F type NBL (F>UF) were mapped. The chromosomal loci at 1q21–q25, 2p24 and 17q21–q25 have been reported as the regions with amplification or gain of additional chromosomal segments (Plantaz *et al.*, 1997; Bown *et al.*, 1999; Hirai *et al.*, 1999). Two differentially expressed genes (F<UF) were mapped to 17q23.2–q23.3 and 2p24.2–p24.3, but no such genes were mapped in the 1q arm.

### *Molecular analysis of the identified genes*

To confirm the reliability of our screening system, we performed quantitative real-time RT–PCR of the differentially expressed genes by using 116 primary NBL samples. *FOG-2/Nbla03139*, one of those genes (Figure 2 and Table 4), showed significantly higher levels of mRNA expression in average in the tumors with favorable prognosis than in those with unfavorable prognosis, although their expression values ranged widely (Figure 4). Seven NBLs with favorable phenotype (>300 e.u., Figure 4) exhibited markedly high expression; however, we could not find any other specific clinical characteristics for these cases. Svensson *et al.* (1999) reported that *FOG-2* expression was observed in the heart, brain and testis of the adult mouse, and in the neural epithelium, heart, urogenital ridge and gonad in developing mouse embryo. We also investigated the *FOG-2* expression in the parasagittal section of the adult mouse brain (7 weeks) and found that it was expressed in a limited part such as dentate gyrus in hippocampal formation (CA3-CA4) and granule cell layer in the cerebellum (data not shown). Therefore, in addition to the role in heart morphogenesis (Tevosian *et al.*, 1999), FOG-2 was suggested to play some role in the developing neurons as well as in NBLs. Other novel genes with differential expression between the NBL subsets are currently being subjected to similar analyses.

**Table 4** Differentially expressed genes between favorable and unfavorable neuroblastomas

| | *Nbla no.* | *Homology search* | *Category* | *Chr. location* |
|---|---|---|---|---|
| F>U | Nbla-00022 | Dihydropyrimidinase-related protein-1 (DRP-1) | A | 4p16.1–15 |
| | Nbla-00080 | Doublecortin | A | Xq22.3–q23 |
| | Nbla-00086 | Small GTPase RAB6B (RAB6B) | A | 3q21–q23 |
| | Nbla-00126 | Homeotic regulator homolog MAB21 | A | |
| | Nbla-00134 | MTG8-like protein MTGR1b | A | 20q11.21–q11.23 |
| | Nbla-00178 | Arg/Abl-interacting protein ArgBP2a | A | 4q |
| | Nbla-00185 | Phosphatidylinositol 3-kinase p45 subunit | A | |
| | Nbla-00226 | Mouse Hox 3.5 | A | |
| | Nbla-00461 | Dihydropyrimidinase-related protein-3 (DRP-3) | A | 5q32 |
| | Nbla-00483 | WSB-1 | A | |
| | Nbla-00494 | GTP-binding protein (rab 3C) | A | |
| | Nbla-00665 | Adenylyl cyclase-associated protein homolog CAP2 | A | 6 |
| | Nbla-00697 | Neurexophilin 1 (Nxph 1) | A | |
| | Nbla-00715 | Camk-2 mRNA for $Ca^{2+}$/calmodulin-dependent protein kinase II beta subunit | A | |
| | Nbla-00766 | Neuronal nicotinic acetylcholine receptor alpha-7 subunit | A | 15q14 |
| | Nbla-00778 | Trio | A | 5p15.1–p14 |
| | Nbla-00856 | Neuron-specific growth-associated protein SCG10 | A | |
| | Nbla-02985 | Dihydropyrimidinase-related protein-2 (DRP-2) | A | 8p21 |
| | Nbla-03139 | FOG-2 | A | 8 |
| | Nbla-03551 | SPOP | A | 17 |
| | Nbla-03678 | EWS | A | 22q12 |
| | Nbla-03932 | Beta-adrenergic receptor kinase 2 (beta-ARK2) | A | 22q11 |
| | Nbla-03949 | Stathmin-like-protein splice variant RB3′ | A | |
| | Nbla-10272 | Protein kinase C zeta | A | 1p36.33–p36.2 |
| | Nbla-10314 | PAK-interacting exchange factor beta | A | 13 |
| | Nbla-10919 | Double cortin- and calmodulin kinase-like 1; DCAMKL1 | A | 13q13 |
| | Nbla-11211 | Islet cell antigen ICA-512 (putative tyrosine phosphatase) | A | 2q35–q36.1 |
| | Nbla-12117 | Trithorax homolog MLLT4 | A | 6q27 |
| | Nbla-12156 | testis-specific cAMP-dependent protein kinase catalytic subunit (C-beta isoform) (PRKACB) | A | 1p36.1 |
| | Nbla-12173 | Platelet-activating factor acetylhydrolase, isoform Ib, alpha subunit (PAFAH1B1). | A | 17p13.3 |
| | Nbla-12182 | Protein phosphatase 1G (formerly 2C) | A | |
| | Nbla-00015 | Protein regulating cytokinesis 1 (PRC 1) | | C15 |
| | Nbla-00453 | PCTAIRE-2 for serine/threonine protein kinase | C | |
| | Nbla-10634 | Tyrosine phosphatase CDC25B | C | 20p13 |
| | Nbla-12080 | CDC2L5 protein kinase | C | |
| | Nbla-12196 | bcl-1 /PRAD1/cyclin | C | 11p13 |
| | Nbla-00002 | Protocadherin gamma A8 short form | D | 5q31 |
| | Nbla-00045 | Laminin alpha4 | D | 6q21 |
| | Nbla-00120 | Cadherin | D | 5q31 |
| | Nbla-00863 | Fibronectin receptor beta subunit | D | 10p11.2 |
| | Nbla-03068 | Peripherin (PRPH) | D | 12q12–q13 |
| | Nbla-03361 | Arp2/3 protein complex subunit p16-Arc (ARC16) | D | |
| | Nbla-10522 | Protocadherin alpha 9 (PCDH-alpha9) | D | 5q31 |
| | Nbla-11090 | Dynein light-chain-A | D | 3 |
| | Nbla-00405 | PHD Finger 1 (PHF1) | E | 6p21.3 |
| | Nbla-00407 | RNA polymerase III largest subunit (hRPC155) | E | |
| | Nbla-00505 | Monocytic leukemia zinc-finger protein (MOZ) | E | 8p11 |
| | Nbla-00534 | CHD2 | E | 15q26 |
| | Nbla-00554 | AP-2 beta transcription factor | E | 6p12 |
| | Nbla-00687 | Top2 for DNA topoisomerase II | E | 3p24 |
| | Nbla-03444 | Transcription elongation factor TFIIS-1. | E | 3p22–p21.3 |
| | Nbla-04244 | ISL-1 (Islet-1) | E | 5q |
| | Nbla-10317 | CUTL1 | E | 7q22 |
| | Nbla-10473 | Androgen-induced prostate proliferative shutoff-associated protein (AS3) | E | |
| | Nbla-10516 | TSC-22 | E | 13q14 |
| | Nbla-10805 | CRE-BP1 transcription factor | E | 2q32 |
| | Nbla-11011 | HSTAFII10 | E | 10q24–q25.2 |
| | Nbla-11047 | Homeodomain protein (OG12) SHOX2 | E | 3q25–26.1 |
| | Nbla-11288 | Bromodomain adjacent to zinc-finger domain, 2B (BAZ2B) | E | 2q23-q24 |
| | Nbla-11543 | ZBP-89 zinc-finger protein 148 | E | 3q21 |
| | Nbla-11714 | TCF4, transcription factor ITF-2 | E | 18q21.1 |
| | Nbla-11741 | Chromodomain helicase DNA-binding protein, 4 (CHD4) | E | 12p13 |
| | Nbla-12052 | HIRIP3 | E | 22q11 |
| | Nbla-12087 | RNA helicase-related protein | E | |
| | Nbla-12111 | Zinc fingers and homeoboxes 1 (ZHX1) | E | 8q |
| | Nbla-11116 | Chromosome-associated protein-E (hCAP-E) | F | 9 |

Table 4 Continued

| | Nbla no. | Homology search | Category | Chr. location |
|---|---|---|---|---|
| F>U | Nbla-00028 | Cytosolic asparaginyl-tRNA synthetase | G | |
| | Nbla-00132 | Cytochrome *b561* | G | 17q11–qter |
| | Nbla-00198 | Dipeptidyl aminopeptidase-like protein | G | 7q |
| | Nbla-00310 | Polyubiquitin | G | 12q24 |
| | Nbla-00588 | Vacuolar-type H( + ) ATPase 115 kDa subunit | G | 17q21 |
| | Nbla-00727 | *Rattus norvegicus* rexo70 | G | |
| | Nbla-03169 | *Rattus norvegicus* rsec5 | G | |
| | Nbla-03296 | Ubiquitin-conjugating enzyme UbcH7 | G | 22q11.2-q13.1 |
| | Nbla-03439 | Guanine nucleotide-exchange protein (ARF-GEP1) | G | 8q13 |
| | Nbla-04240 | Glutaminyl-tRNA synthetase | G | 3p21.3–p21.1 |
| | Nbla-10139 | Calumein (Calu) | G | 7q32 |
| | Nbla-10390 | Apg12 | G | 5q21–22 |
| | Nbla-10667 | Homolog of yeast ubiquitin-protein ligase Rsp5 | G | 18q |
| | Nbla-11270 | Aczonin | G | 7q11.23–q22.1 |
| | Nbla-11674 | SUMO-1-specific protease (SSP1) | G | 6q13–q14.3 |
| | Nbla-11768 | Polyadenylate-binding protein | G | |
| | Nbla-11836 | ATP-dependent metalloprotease YME 1 L. | G | 10p14 |
| | Nbla-12036 | Solute carrier family 11 (proton-coupled divalent metal ion transporters) | G | 2q32 |
| | Nbla-12123 | Clk-associating RS-cyclophilin (CYP) | G | 2 |
| | Nbla-12177 | HNOP56 | G | |
| | Nbla-00065 | K+ channel beta 2 subunit | H | 1p36.3 |
| | Nbla-00258 | CIRP | H | 19p13.3 |
| | Nbla-00269 | Dopamine beta-hydroxylase type a (DBH) | H | 9q34 |
| | Nbla-00664 | GTP cyclohydrolase 1 | H | 14q22.1–q22.2 |
| | Nbla-00775 | UCP3 | H | 11q13 |
| | Nbla-03037 | Cytoplasmic aminopeptidase P (APP) | H | 10q25.3 |
| | Nbla-03654 | alpha-L-fucosidase | H | 1p34 |
| | Nbla-03664 | K+ channel beta subunit | H | 3q26.1 |
| | Nbla-03819 | Monoamine oxidase type A (MAO) | H | Xp11.4–p11.3 |
| | Nbla-03905 | Chaperonin protein (Tcp20) | H | |
| | Nbla-04104 | Na,K-ATPase alpha-1 subunit | H | 1p13–p11 |
| | Nbla-10614 | HUMHSF2 Human heat-shock factor 2 (HSF2) | H | 6pter–p25.1 |
| | Nbla-10934 | Solute carrier family 25, SLC25A13 | H | 7q21.3 |
| | Nbla-12011 | HSP90 co-chaperone (progesterone receptor complex p23) | H | |
| | Nbla-12192 | Lactoylglutathione lyase | H | 6p21.3–p21.1 |
| | Nbla-12203 | Vacuolar proton pump subunit 1(clathrin-coated vesicle/synaptic vesicle proton pump 116 kDa subunit) | H | |
| | Nbla-00495 | Pescadillo | I | 22q12.1 |
| | Nbla-02902 | Erythroblast macrophage protein EMP | I | |
| | Nbla-03824 | Imidazoline receptor antisera-selected protein | I | |
| | Nbla-04263 | Butyrophilin (BTF4) | I | 6p |
| | Nbla-10394 | Amyloid precursor-like protein 1 | I | 19q13.1 |
| | Nbla-10842 | NIPSNAP1 | I | 22q12.2 |
| | Nbla-11694 | AF1q | I | 1q21 |
| F<U | Nbla-03566 | DDX1 | G | 2p24 |
| | Nbla-10449 | NLRR-1 leucine-rich-repeat protein | D | 3p |

Category: A = cell signaling, B = cytokine, growth factor, hormones, C = cell cycle, D = cell structure, adhesion, movement, E = transcription, F = DNA replication, DNA repair, DNA synthesis, G = protein synthesis, process, transport, turn over, H = homeostasis, heat-shock protein, metabolic enzymes, I = others, unknown

## Discussion

For understanding the molecular basis of neuroblastoma, accumulation and collection of a large number of genes, which may be involved in the neural crest development, neuronal cell growth, differentiation and programmed cell death, is very useful. The recent progress of the Human Genome Project has enabled us to take such an approach in the field of cancer research.

In this study, we generated oligo-capping cDNA libraries from the primary NBL subsets with different clinicobiological characteristics to clone randomly the cDNAs expressed. Our extensive screening for the differentially expressed genes between F and UF subsets of NBL has identified at least 305 such genes, including 194 novel genes with unknown function.

### *Neuroblastoma cDNA libraries*

We have identified the genes with an unknown function in nearly half (40%) of the total 4654 clones from the cDNA libraries we generated, which correspond to 1152 independent novel genes. The expression profile of each library seemed to be quite different supposed from the expression pattern of the known genes. The UF library

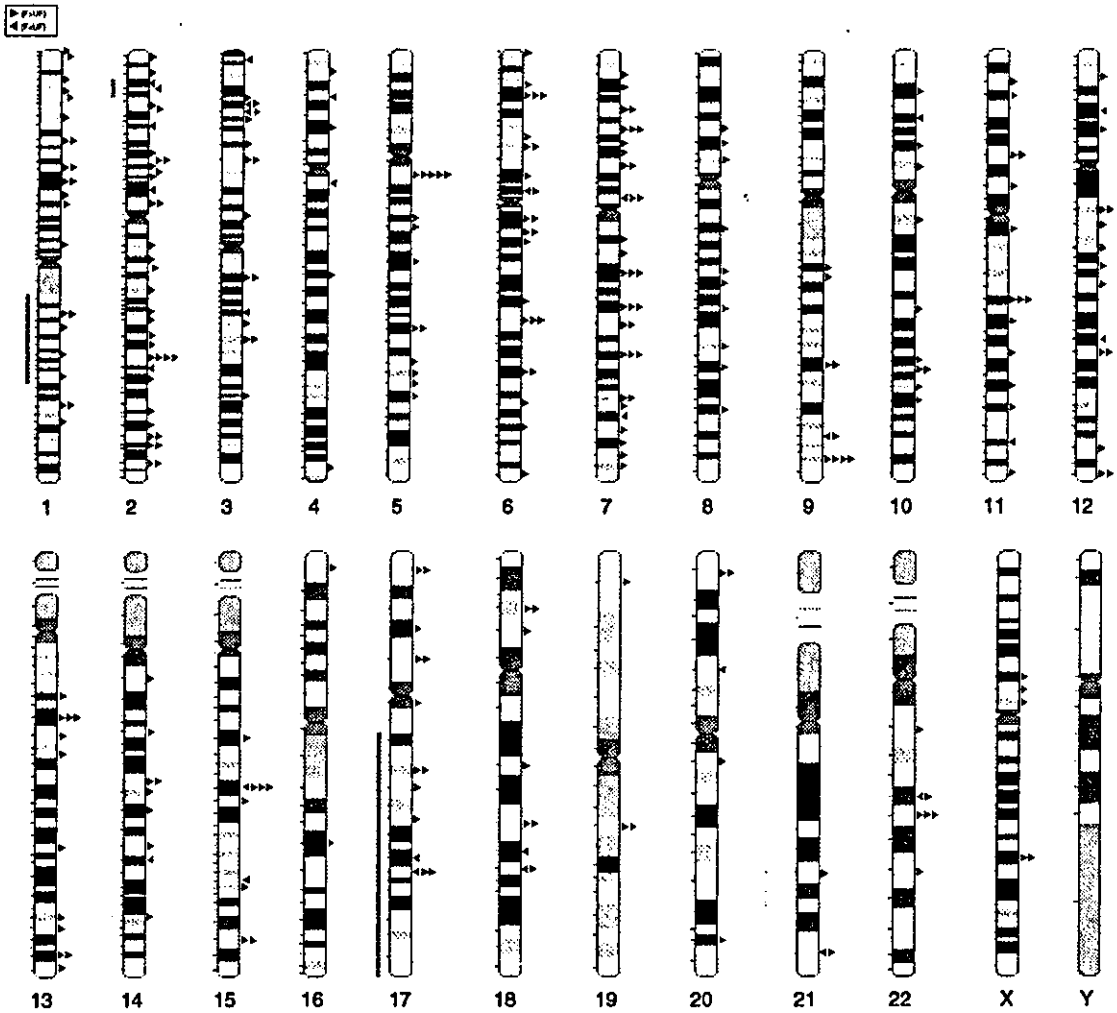


**Figure 3** Chromosomal location of the genes differentially expressed between the F- and UF-NBL subsets. Arrowheads facing left show the genes preferentially expressed in favorable NBLs, and those facing right show the genes preferentially expressed in unfavorable NBLs

showed a profile of enhanced protein synthesis, and also a high frequency of *DDX-1* gene. However, we have found that neither *MYCN* nor *TRKA* genes in the clones sequenced. Some of the explanations are that the cDNAs with the specific sequences such as GC-rich regions may be difficult to clone in our oligo-capping cloning system due to an unknown reason and that some genes with GC-rich sequences cannot be DNA sequenced. We indeed missed 411 cDNAs due to impossible sequencing.

The lineup of known genes in the F and UF libraries, especially of abundantly expressed genes, indicated that NBLs had a typical pattern of neuronal gene expression profiles. Bodymap (http://bodymap.ims.u-tokyo.ac.jp/) is a human gene expression database, collecting quantitative and qualitative information on gene expression in various tissues or cell types (Okubo *et al.*, 1992). It utilized a neuroblastoma cell line CHP134 (with *MYCN* amplification) as a source of neuronal gene expression. In this map, the expression of *14-3-3 epsilon* and *N-cadherin* was also shown to be neuron-specific. However, our present study has added a large number of neuronal genes, including *P311* and *SCG10* as well as many novel genes.

### *Screening of the differentially expressed genes*

For screening the differentially expressed genes, the methods such as differential display-PCR and serial analysis of gene expression (SAGE) have been applied (McClelland *et al.*, 1995; Velculescu *et al.*, 2000). These techniques are advantageous because of high throughput and low cost. However, the cloned materials and obtained sequences are very short in length so that it is difficult to obtain a full-length cDNA that is ready for functional analysis. Since our final goal is to identify the important genes expressed differentially between the different subsets of NBL and to clarify their function, we have decided to introduce the method to clone directly as many genes as possible from the cDNA libraries constructed from the primary NBLs. In addition, we have performed semi-quantitative RT–PCR to screen for the differentially expressed genes by using 16 F and 16 UF primary NBL samples. Our

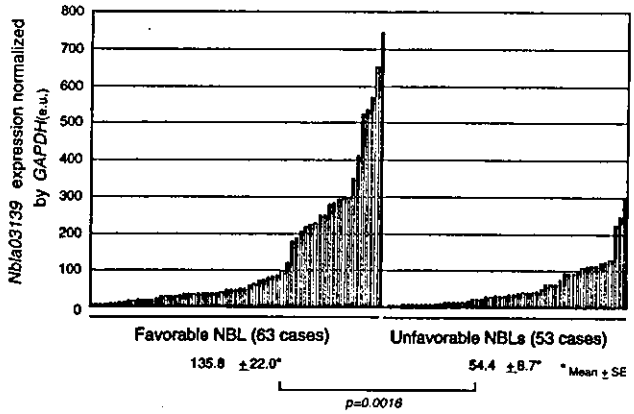


**Figure 4** Characterization of the *Nbla03139/FOG-2* gene. Expression analysis of the *FOG-2* gene in 116 primary NBL samples using quantitative real-time RT–PCR. A total of 63 favorable and 53 unfavorable NBLs were analysed. The vertical axis shows expression units relative to the value of *GAPDH* expression. The mean values of the expression level in favorable and unfavorable NBLs are shown at the bottom of the graph

present approach is neither high throughput nor low cost, but the results are consistent. As a result, we have identified 305 independent genes expressed differentially between F and UF subsets, which is a huge number that has so far not been reported. All these genes can be good candidates of new biological and prognostic markers of NBL. Detailed analyses of several differentially expressed genes from this point of view will be described elsewhere (Kawamoto *et al.*, 2003). The genes related to catecholamine metabolism such as *DBH* and *MAO* may also become new prognostic indicators. The down-regulation of their expression in the UF tumors seems to support the previously proposed hypothesis that the advanced NBLs with *MYCN* amplification are dopaminergic with the blockade of a metabolic process from dopamine to noradrenaline (Nakagawara *et al.*, 1988, 1990). Transcription factors and their regulators, such as homeodomain-containing transcription factors and chromatin-modifying molecules, are also important for understanding the biology of NBL subsets. Many other genes that are regulated by those molecules may also be included in the differentially expressed genes.

### *Differential RT–PCR analysis of methylation- and acetylation-related genes*

Our results have shown that the number of genes expressed at high levels in the F subset is about 10 times larger than that in the UF subset (278 *vs* 27 genes). The following three explanations can be given for this. Firstly, we have used *GAPDH* expression as a control to adjust and standardize cDNA concentration of F and UF samples because most of the papers so far published have utilized *GAPDH* as a standard. In this case, there occurs a possibility that the relatively high levels of *GAPDH* expression is indicated in the UF samples, giving the relatively decreased values of cDNA expression. However, we have used another control gene *β-actin* that has given a result similar to *GAPDH*. Secondly, Boon *et al.* (2001) have reported that the overexpression of *MYCN* induces the expression of a large set of genes, which involves those related to ribosome biogenesis and protein synthesis. In our study, those genes are also frequently found in the UF library, but they have been excluded from our further study. Thirdly, the yet unknown mechanisms regulating the gene expression may be present between the two subsets. For example, the epigenetic regulation, including chromosomal methylation or histone acetylation, could be present. Therefore, in the preliminary study, we have examined whether or not the genes regulating DNA methylation or histone acetylation are differentially expressed between F and UF subsets of NBL. However, none of the methylation-related genes (*DNMT1,2,3*, *MBD1,2,3,4* and *MeCP2*) have displayed differential expression (Furuya *et al.*, unpublished data). On the other hand, some members of histone acetylation-related genes (*CBP* and *HAT1*) have shown a pattern of differential expression to a certain extent, suggesting the presence of different epigenetic regulation in the gene expression between the subsets (Furuya *et al.*, in preparation). Several recent reports have shown that the epigenetically regulated genes in cancers and other hereditary diseases often cluster in continuous regions (Mitsuya *et al.*, 1999; Okutsu *et al.*, 2000; Ono *et al.*, 2001). In our present data, some clusters of the F>UF genes have been found in chromosomes 2, 5, 6, 7, 9, 11, 13, 15 and 22, suggesting the existence of the epigenetically regulated chromosomal loci in NBLs.

In conclusion, our NBL cDNA project has provided us with 2313 known genes and 1799 novel genes with an unknown function, among which 111 known and 194 novel genes are differentially expressed between F and UF subsets of NBL. This huge number of cDNA resources may become an important tool to unveil the molecular mechanism of the enigmatic clinical behavior of NBL, as well as to develop new diagnostic and therapeutic strategies against the aggressive tumors in the future. We are currently expanding this cDNA project to the stage 4s NBL and applying the clones to the cDNA microarray system.

## Materials and methods

### *Tissues and cell lines*

Fresh, frozen tumor tissues were sent to the Division of Biochemistry, Chiba Cancer Center Research Institute, from various hospitals in Japan. The tumors were staged according to the International Neuroblastoma Staging System. (stages 1 and 2, localized neuroblastomas; stages 3 and 4, locally and regionally growing and distantly metastatic neuroblastomas; and stage 4s, neuroblastomas in children under 1 year of age, with metastases restricted to the skin, liver and bone marrow, usually regressing spontaneously) (Brodeur *et al.*, 1993). In Japan, a mass screening program for infants at the age of 6 months has been performed since 1984. Patients found by this screening have been mostly classified into the early stage of the disease, although a small proportion had unfavorable prognoses (Sawada *et al.*, 1984). A total of 116 neuroblastoma samples (39 were classified as being stage 1, 18 as stage 2, 11 as

stage 3, 42 as stage 4 and six as stage 4s) containing 61 patients found by mass screening were used in this study. The informed consents were obtained in each institution or hospital. The tumors were divided into two subsets, one with a favorable prognosis and the other with an unfavorable prognosis, according to the clinical and biological markers (Seeger *et al.*, 1985; Bartram and Berthold, 1987; Nakagawara *et al.*, 1987, 1992, 1993; Slavc *et al.*, 1990; Look *et al.*, 1991; Brodeur *et al.*, 1993). High molecular weight DNA and total RNA of these samples were prepared as described previously (Ichimiya *et al.*, 1999).

*cDNA library construction*

Oligo-capping cDNA libraries (Maruyama and Sugano, 1994; Suzuki *et al.*, 1997) were constructed from the mixture of three-stage 1 NBL frozen tissues with a single copy of *MYCN* (favorable subset) and from that of three NBL frozen tissues in stages 3 and 4 with *MYCN* amplification (unfavorable subset). They were approved by the institutional review board.

*Sequencing and classification of cDNA clones*

Independent clones from two subsets of libraries were randomly picked up and sequenced from both ends. The end sequences of 2410 clones obtained from the favorable NBL library and those of 2244 clones from the unfavorable NBL library were then homology searched against public databases (Genbank release 122, January 2001) using Cybergate sequence classification system (Dynacom Inc.) and bundled into gene clusters by assembling sequences. The end sequences that included a novel sequence were submitted to DDBJ/GenBank nucleotide database (Accession no. AU252405–AU254042).

*Differential screening of the genes by semiquantitative RT–PCR*

Typical 16 samples from each NBL subset were selected as PCR templates to screen for the differentially expressed genes. All 16 tumors with the favorable biology were defined as stage 1 NBLs with no *MYCN* amplification, but with a high expression of *TrkA*. The 16 tumors with unfavorable biology were in stage 3 or 4, exhibiting *MYCN* amplification and low *TrkA* expression. The differential expression of the genes between the NBL subsets was confirmed at least twice using semiquantitative RT–PCR. The individual gene-specific PCR primer sequences were determined by using Primer3 program (provided at Washington University). For cDNA templates, 5 $\mu$g of total RNA was converted into cDNA using random primers (Takara, Otsu, Japan) with SuperScript II RNaseH$^-$ reverse transcriptase (Gibco BRL, Rockville, MD, USA). Those cDNAs were at first amplified with Cy5-labeled *GAPDH* primers in 25 cycles and the amounts of PCR products were measured by ALF Express™ sequencer and normalized. The amplification was performed as follows: 35 cycles of 94°C for 30 s, 61°C for 15 s and 72°C for 60 s, and the final extension was at 72°C for 5 min, using a Perkin Elmer Thermalcycler 9700 (Perkin-Elmer, Foster City, CA, USA). The PCR products were run on 2% agarose gels and stained with ethidium bromide.

*Quantification of genes expression by real-time RT–PCR*

Real-time RT–PCR was performed in triplicates to quantify the amounts of genes expressed in the primary neuroblastomas (Abe *et al.*, 1999; Inoue *et al.*, 1999). The reaction was performed using a PCR core reagent kit with an ABI 7700 sequence detector system (Perkin-Elmer, Foster City, CA, USA). Five micrograms of total RNA was converted into cDNA using random primers with SuperScript II reverse transcriptase and diluted by 20-fold. The reaction mixtures (25 $\mu$l) contained 2 $\mu$l of cDNA solution, 2.5 $\mu$l of 10 × Taq Man buffer A, 200 $\mu$M dATP, 200 $\mu$M dCTP, 200 $\mu$M dGTP, 400 $\mu$M dUTP, 3.5 mM MgCl2, 300 nM forward primer, 300 nM reverse primer, 300 nM Taq Man probe, 0.625 U of Ampli Taq Gold DNA polymerase and 0.25 U of Amp Erase uracil *N*-glycosylase (UNG) (Perkin-Elmer). The thermal cycling conditions were as follows: initial activation of UNG at 50°C for 2 min followed by activation of Ampli Taq Gold and inactivation of UNG at 95°C for 10 min, and subsequently, 40 cycles of amplification were performed at 95°C for 15 s and 60°C for 1 min. The amount of *GAPDH* mRNA in all samples was measured by real-time RT–PCR as a control using Taq Man *GAPDH* Control Reagents (Roche Molecular Systems, Inc., Branchburg, NJ, USA).

**Acknowledgements**
We are grateful to the hospitals and institutions who provided us with the surgical specimens. We thank Shiho Hamano for helping with quantitative PCR analysis as well as statistical analysis, and Emiko Kojima, Natsue Kitabayashi, Hisae Murakami, Naoko Sugimitsu and Yuki Nakamura for technical support. We also appreciate helpful discussions with Masayuki Fukumura, Kenji Kadomastu, Minenobu Okayama and Hiroki Kurihara, and the encouragement given by Dr Naohiko Seki. This work was supported by a fund from Hisamitsu Pharmaceutical Company, and in part by a grant from grant-in-aid for Scientific Research on Priority Areas (C) 'Medical Genome Science' from the Ministry of Education, Culture, Sports, Science and Technology of Japan.

**References**

Abe A, Inoue K, Tanaka T, Kato J, Kajiyama N, Kawaguchi R, Tanaka S, Yoshiba M and Kohara M. (1999). *J. Clin. Microbiol.*, **37**, 2899–2903.

Amler LC, Schurmann J and Schwab M. (1996). *Genes Chromosomes Cancer*, **15**, 134–137.

Anderson DJ and Axel R. (1985). *Cell*, **42**, 649–662.

Bartram CR and Berthold F. (1987). *Eur. J. Pediatr.*, **146**, 162–165.

Boon K, Caron HN, van Asperen R, Valentijn L, Hermus MC, van Sluis P, Roobeek I, Weis I, Voute PA, Schwab M and Versteeg R. (2001). *EMBO J.*, **20**, 1383–1393.

Bown N, Cotterill S, Lastowska M, O'Neill S, Pearson AD, Plantaz D, Meddeb M, Danglot G, Brinkschmidt C, Christiansen H, Laureys G and Speleman F. (1999). *N. Engl. J. Med.*, **340**, 1954–1961.

Brodeur GM and Nakagawara A. (1992). *Am. J. Pediatr. Hematol. Oncol.*, **14**, 111–116.

Brodeur GM, Pritchard J, Berthold F, Carlsen NL, Castel V, Castelberry RP, De Bernardi B, Evans AE, Favrot M, Hedborg F, Kaneko M, Tsuchida Y, Philip T, Ronald B, and Voute PA. (1993). *J. Clin. Oncol.*, **11**, 1466–1477.

Brodeur GM, Seeger RC, Schwab M, Varmus HE and Bishop JM. (1984). *Science*, **224**, 1121–1124.

Caron H, Peter M, van Sluis P, Speleman F, de Kraker J, Laureys G, Michon J, Brugieres L, Voute PA, Westerveld A and Versteeg R. (1995). *Hum. Mol. Genet.*, **4**, 535–539.

Hamajima N, Matsuda K, Sakata S, Tamaki N, Sasaki M and Nonaka M. (1996). *Gene*, **180**, 157–163.
Hirai M, Yoshida S, Kashiwagi H, Kawamura T, Ishikawa T, Kaneko M, Ohkawa H, Nakagawara A, Miwa M and Uchida K. (1999). *Genes Chromosomes Cancer*, **25**, 261–269.
Hirano S, Nose A, Hatta K, Kawakami A and Takeichi M. (1987). *J. Cell Biol.*, **105**, 2501–2510.
Hishiki T, Nimura Y, Isogai E, Kondo K, Ichimiya S, Nakamura Y, Ozaki T, Sakiyama S, Hirose M, Seki N, Takahashi H, Ohnuma N, Tanabe M and Nakagawara A. (1998). *Cancer Res.*, **58**, 2158–2165.
Ichimiya S, Nimura Y, Kageyama H, Takada N, Sunahara M, Shishikura T, Nakamura Y, Sakiyama S, Seki N, Ohira M, Kaneko Y, McKeon F, Caput D and Nakagawara A. (1999). *Oncogene*, **18**, 1061–1066.
Inoue K, Yoshiba M, Sekiyama K and Kohara M. (1999). *J. Hepatol.*, **30**, 801–806.
Kawamoto T, Ohira M, Hamano S, Hori T and Nakagawara A. (2003). *Int. J. Oncol.*, **22**, 815–822.
Look AT, Hayes FA, Shuster JJ, Douglass EC, Castleberry RP, Bowman LC, Smith EI and Brodeur GM. (1991). *J. Clin. Oncol.*, **9**, 581–591.
Maruyama K and Sugano S. (1994). *Gene*, **138**, 171–174.
Matsumoto K, Wada RK, Yamashiro JM, Kaplan DR and Thiele CJ. (1995). *Cancer Res.*, **55**, 1798–1806.
McClelland M, Mathieu-Daude F and Welsh J. (1995). *Trends Genet.*, **11**, 242–246.
McConnell JE, Armstrong JF, Hodges PE and Bard JB. (1995). *Dev. Biol.*, **169**, 218–228.
Mitsuya K, Meguro M, Lee MP, Katoh M, Schulz TC, Kugoh H, Yoshida MA, Niikawa N, Feinberg AP and Oshimura M. (1999). *Hum. Mol. Genet.*, **8**, 1209–1217.
Nakagawara A. (1998). *Hum. Cell*, **11**, 115–124.
Nakagawara A, Arima M, Azar CG, Scavarda NJ and Brodeur GM. (1992). *Cancer Res.*, **52**, 1364–1368.
Nakagawara A, Arima-Nakagawara M, Scavarda NJ, Azar CG, Cantor AB and Brodeur GM. (1993). *N. Engl. J. Med.*, **328**, 847–854.
Nakagawara A, Azar CG, Scavarda NJ and Brodeur GM. (1994). *Mol. Cell. Biol.*, **14**, 759–767.
Nakagawara A, Ikeda K, Higashi K and Sasazuki T. (1990). *Surgery*, **107**, 43–49.
Nakagawara A, Ikeda K and Tasaka H. (1988). *J. Pediatr. Surg.*, **23**, 346–349.
Nakagawara A, Ikeda K, Tsuda T and Higashi K. (1987). *J. Pediatr. Surg.*, **22**, 895–898.
Nakagawara A, Milbrandt J, Muramatsu T, Deuel TF, Zhao H, Cnaan A and Brodeur GM. (1995). *Cancer Res.*, **55**, 1792–1797.
Noguchi T, Akiyama K, Yokoyama M, Kanda N, Matsunaga T and Nishi Y. (1996). *Genes Chromosomes Cancer*, **15**, 129–133.
Okubo K, Hori N, Matoba R, Niiyama T, Fukushima A, Kojima Y and Matsubara K. (1992). *Nat. Genet.*, **2**, 173–179.
Okutsu T, Kuroiwa Y, Kagitani F, Kai M, Aisaka K, Tsutsumi O, Kaneko Y, Yokomori K, Surani MA, Kohda T, Kaneko-Ishino T and Ishino F. (2000). *J. Biochem.*, **127**, 475–483.
Ono R, Kobayashi S, Wagatsuma H, Aisaka K, Kohda T, Kaneko-Ishino T and Ishino F. (2001). *Genomics*, **73**, 232–237.
Plantaz D, Mohapatra G, Matthay KK, Pellarin M, Seeger RC and Feuerstein BG. (1997). *Am. J. Pathol.*, **150**, 81–89.
Sawada T, Hirayama M, Nakata T, Takeda T, Takasugi N, Mori T, Maeda K, Koide R, Hanawa Y, Tsunoda A, Shimizu K, Nagahara N and Yamamoto K. (1984). *Lancet*, **2**, 271–273.
Seeger RC, Brodeur GM, Sather H, Dalton A, Siegel SE, Wong KY and Hammond D. (1985). *N. Engl. J. Med.*, **313**, 1111–1116.
Slavc I, Ellenbogen R, Jung WH, Vawter GF, Kretschmar C, Grier H and Korf BR. (1990). *Cancer Res.*, **50**, 1459–1463.
Studler JM, Glowinski J and Levi-Strauss M. (1993). *Eur. J. Neurosci.*, **5**, 614–623.
Suzuki Y, Yoshitomo-Nakagawa K, Maruyama K, Suyama A and Sugano S. (1997). *Gene*, **200**, 149–156.
Svensson EC, Tufts RL, Polk CE and Leiden JM. (1999). *Proc. Natl. Acad. Sci. USA*, **96**, 956–961.
Taguchi A, Wanaka A, Mori T, Matsumoto K, Imai Y, Tagaki T and Tohyama M. (1996). *Brain Res. Mol. Brain Res.*, **35**, 31–40.
Takita J, Hayashi Y, Kohno T, Yamaguchi N, Hanada R, Yamamoto K and Yokota J. (1997). *Cancer Res.*, **57**, 907–912.
Tevosian SG, Deconinck AE, Cantor AB, Rieff HI, Fujiwara Y, Corfas G and Orkin SH. (1999). *Proc. Natl. Acad. Sci. USA*, **96**, 950–955.
Velculescu VE, Vogelstein B and Kinzler KW. (2000). *Trends Genet.*, **16**, 423–425.

THE JOURNAL OF BIOLOGICAL CHEMISTRY
© 2005 by The American Society for Biochemistry and Molecular Biology, Inc.

Vol. 280, No. 17, Issue of April 29, pp. 16665–16675, 2005
Printed in U.S.A.

# Identification of Protein Kinase A Catalytic Subunit β as a Novel Binding Partner of p73 and Regulation of p73 Function*

Received for publication, December 20, 2004, and in revised form, January 31, 2005
Published, JBC Papers in Press, February 21, 2005, DOI 10.1074/jbc.M414323200

**Takayuki Hanamoto‡§, Toshinori Ozaki‡, Kazushige Furuya‡, Mitsuchika Hosoda‡, Syunji Hayashi‡, Mitsuru Nakanishi‡, Hideki Yamamoto‡, Hironobu Kikuchi‡, Satoru Todo§, and Akira Nakagawara‡¶**

*From the ‡Division of Biochemistry, Chiba Cancer Center Research Institute, Chiba 260-8717, Japan and the §Department of General Surgery, Hokkaido University School of Medicine, Kita-ku, Sapporo 060-8638, Japan*

**Post-translational modifications play a crucial role in regulation of the protein stability and pro-apoptotic function of p53 as well as its close relative p73. Using a yeast two-hybrid screening based on the Sos recruitment system, we identified protein kinase A catalytic subunit β (PKA-Cβ) as a novel binding partner of p73. Co-immunoprecipitation and glutathione *S*-transferase pull-down assays revealed that p73α associated with PKA-Cβ in mammalian cells and that their interaction was mediated by both the N- and C-terminal regions of p73α. In contrast, p53 failed to bind to PKA-Cβ. *In vitro* phosphorylation assay demonstrated that glutathione *S*-transferase-p73α-(1–130), which has one putative PKA phosphorylation site, was phosphorylated by PKA. Enforced expression of PKA-Cβ resulted in significant inhibition of the transactivation function and pro-apoptotic activity of p73α, whereas a kinase-deficient mutant of PKA-Cβ had no detectable effect. Consistent with this notion, treatment with H-89 (an ATP analog that functions as a PKA inhibitor) reversed the dibutyryl cAMP-mediated inhibition of p73α. Of particular interest, PKA-Cβ facilitated the intramolecular interaction of p73α, thereby masking the N-terminal transactivation domain with the C-terminal inhibitory domain. Thus, our findings indicate a PKA-Cβ-mediated inhibitory mechanism of p73 function.**

p73 has been identified as a structural and functional homolog of the tumor suppressor p53 (1). p53 and p73 share the same domain organization, consisting of an N-terminal transactivation domain, a central sequence-specific DNA-binding domain, and a C-terminal oligomerization domain. As expected, several pieces of evidence suggest that p73 can bind to the p53-responsive element and transactivate an overlapping set of p53 target genes, thus leading to induction of $G_1$/S cell cycle arrest and apoptosis (1–6). In marked contrast to p53, p73 is expressed as multiple isoforms arising from alternative splicing of the primary p73 transcript (p73α, p73β, p73γ, p73δ, p73ε, p73η, and p73ζ) termed the TA variant (1, 3, 7–9). These alternatively spliced isoforms vary in their C termini and display different transcriptional and biological properties. Additionally, the ΔN variant (ΔNp73α and ΔNp73β), which is generated by alternative promoter utilization, lacks the N-terminal transactivation domain and exhibits dominant-negative behavior toward wild-type p73 as well as p53 (10–12). Recently, we (14) and others (13, 15) demonstrated that p73 directly transactivates the expression of its own negative regulator (ΔNp73), creating an autoregulatory feedback loop in which both the activity of p73 and the expression of ΔNp73 are regulated. Thus, the pro-apoptotic activity of p73 is determined by the relative expression levels of its TAp73 and dominant-negative ΔNp73 variants in cells.

In sharp contrast to p53, it was initially reported that p73 was not induced by DNA damage (1). However, recent studies demonstrated that, in response to a subset of DNA-damaging agents, p73 is positively regulated by multiple post-translational modifications, including phosphorylation and acetylation. During cisplatin-mediated apoptosis, phosphorylation of p73 at Tyr-99 by the non-receptor tyrosine kinase c-Abl results in an increase in its stability and pro-apoptotic activity (16–18). In addition to c-Abl, the protein kinase Cδ catalytic fragment has the ability to phosphorylate p73 at Ser-289 and contributes to the accumulation of p73 during the apoptotic response to cisplatin treatment (19). It is worth noting that the physical and functional interaction between c-Abl and protein kinase Cδ leads to the cross-activation of their kinase functions (20, 21). Furthermore, the enzymatic activity of Chk1 (checkpoint kinase-1) is enhanced in response to DNA damage (22–24), and Chk1 has the ability to phosphorylate p73 at Ser-47 upon DNA damage, thereby enhancing its transactivation ability and pro-apoptotic activity without affecting the level of total p73 protein, whereas Chk2 has no detectable effect on p73 (25). Alternatively, Zeng *et al.* (26) found that the acetyltransferase p300/CBP (cAMP-responsive element-binding protein-binding protein) interacts with the N-terminal region of p73 and stimulates p73-mediated transcriptional activation and apoptosis. Recently, Costanzo *et al.* (27) reported that doxorubicin treatment induces the p300-mediated acetylation of p73 at Lys-321, Lys-327, and Lys-331 in a c-Abl-dependent manner, which is associated with the efficient recruitment of p73 to the promoter of the apoptotic target gene *p53AIP1*. Additionally, it has been shown that p300-mediated acetylation of p73 results in its significant stabilization in a prolyl isomerase Pin1-dependent manner (28).

To identify cellular protein(s) that could interact with full-length p73α and regulate its function, we screened a human fetal brain cDNA library using a yeast two-hybrid method

* This work was supported in part by a grant-in-aid from the Ministry of Health, Labor, and Welfare for Third Term Comprehensive Control Research for Cancer; a grant-in-aid for scientific research on priority areas from the Ministry of Education, Culture, Sports, Science, and Technology of Japan; and a grant-in-aid for scientific research from the Japan Society for the Promotion of Science. The costs of publication of this article were defrayed in part by the payment of page charges. This article must therefore be hereby marked "*advertisement*" in accordance with 18 U.S.C. Section 1734 solely to indicate this fact.

¶ To whom correspondence should be addressed: Div. of Biochemistry, Chiba Cancer Center Research Inst., 666-2 Nitona, Chuoh-ku, Chiba 260-8717, Japan. Tel.: 81-43-264-5431; Fax: 81-43-265-4459; E-mail: akiranak@chiba-cc.jp.

based on the Sos recruitment system. We report here that protein kinase A catalytic subunit β (PKA-Cβ)[1] bound to p73α in cells, but not to p53, and that their interaction was mediated by the N- and C-terminal regions of p73α. *In vitro* kinase assays revealed that the catalytic subunit of PKA phosphorylated p73α. PKA-Cβ inhibited the p73α-mediated transcriptional activation of the $p21^{WAF1}$ and *Bax* promoters and p73α-dependent apoptosis in response to camptothecin. On the other hand, the kinase-deficient mutant of PKA-Cβ had little effect on p73α. Of note, we found that PKA-Cβ facilitated the intramolecular interaction of p73α. Our results strongly suggest the PKA-Cβ-mediated phosphorylation and intramolecular interaction of p73 to be a novel inhibitory mechanism of p73 function.

## EXPERIMENTAL PROCEDURES

*Cell Culture and Cell Lines*—SV40-transformed African green monkey kidney cells (COS-7) were grown in Dulbecco's modified Eagle's medium supplemented with 10% heat-incubated fetal bovine serum (Invitrogen), 100 IU/ml penicillin, and 100 μg/ml streptomycin. p53-deficient human lung carcinoma H1299 cells were maintained in RPMI 1640 medium supplemented with 10% heat-incubated fetal bovine serum and antibiotic mixture. The cells were cultured at 37 °C in a water-saturated atmosphere of 95% air and 5% $CO_2$.

*Transient Transfection*—COS-7 cells grown to 50–70% confluence in 60-mm dishes were transfected with the indicated expression plasmids using FuGENE 6 transfection reagent (Roche Applied Science) following the protocol recommended by the manufacturer. H1299 cells transfection was performed using Lipofectamine 2000 transfection reagent (Invitrogen) according to the manufacturer's instructions.

*Yeast Two-hybrid Screening*—The CytoTrap two-hybrid system was purchased from Stratagene (La Jolla, CA). The cDNA encoding the full-length open reading frame of human p73α was amplified by PCR using pcDNA3-p73α as template. The PCR product, which was produced by additional upstream 5′-BamHI and downstream 3′-SalI restriction sites, was digested completely with BamHI and SalI; purified on agarose gel; and directly inserted in-frame into the identical restriction sites of pSos to give pSos-p73α. The resulting pSos-p73α"bait" plasmid was used to identify the cDNA encoding the p73α-binding protein from a human fetal brain cDNA library cloned into the pMyr plasmid (Stratagene). The screening was carried out according to the manufacturer's instructions. Briefly, a temperature-sensitive yeast strain (cdc25Hα) was cotransformed with pSos-p73α and the cDNA library using the lithium acetate/heat shock procedure as described previously (29). Transformants were allowed to grow on selection medium containing glucose for 2 days at 25 °C and then transferred onto selection medium containing galactose. Plasmid DNAs were isolated from the colonies exhibiting galactose-dependent growth at 37 °C and transformed into *Escherichia coli*. Finally, the nucleotide sequences of the positive cDNA clones were determined by the dideoxy terminator cycle sequencing using an ABI automated DNA sequencer (Applied Biosystems, Foster City, CA).

*Western Blot Analysis*—Transfected cells were washed twice with phosphate-buffered saline (PBS) and lysed in ice-cold lysis buffer A (25 mM Tris-Cl (pH 7.5), 137 mM NaCl, 2.7 mM KCl, and 1% Triton X-100) containing protease inhibitor mixture (Sigma). After a brief sonication, whole cell lysates were centrifuged at 15,000 rpm for 10 min at 4 °C to remove insoluble materials, and the protein concentrations of the supernatants were determined using the Bio-Rad protein assay reagent. Protein samples were boiled in SDS sample buffer for 5 min, resolved by 10% SDS-PAGE, and transferred onto Immobilon-P membranes (Millipore, Bedford, MA). The membranes were blocked overnight with 50 mM Tris-Cl (pH 7.6), 100 mM NaCl, and 0.1% Tween 20 containing 5% nonfat dry milk and then incubated at room temperature for 1 h with anti-FLAG monoclonal antibody (M2, Sigma), anti-green fluorescence protein (GFP) monoclonal antibody (1E4, Medical and Biological Laboratories, Nagoya, Japan), anti-p53 monoclonal antibody (DO-1, Oncogene Research Products, Cambridge, MA), anti-p73 monoclonal antibody (Ab-4, NeoMarkers, Inc., Fremont, CA), anti-$p21^{WAF1}$ monoclonal antibody (Ab-1, Oncogene Research Products), anti-PKA-Cα polyclonal antibody (C-20, Santa Cruz Biotechnology, Inc., Santa Cruz, CA), or anti-PKA-Cβ polyclonal antibody (C-20, Santa Cruz Biotechnology, Inc.), followed by incubation with the corresponding horseradish peroxidase-conjugated secondary antibodies (Jackson ImmunoResearch Laboratories, Inc., West Grove, PA). Following the last wash, horseradish peroxidase-labeled antibodies were detected using an enhanced chemiluminescence detection system (ECL, Amersham Biosciences) according to the manufacturer's instructions.

*Immunoprecipitation and Pull-down Assay*—For immunoprecipitation, cell lysates were prepared in lysis buffer A. Equal amounts of protein extracts were pre-absorbed with protein G-Sepharose beads (Amersham Biosciences) for 1 h at 4 °C, and the precleared lysates were incubated with the indicated antibodies for 2 h at 4 °C, followed by incubation with protein G-Sepharose beads for an additional 1 h at 4 °C. The immune complexes were then washed three times with lysis buffer A, eluted by boiling in SDS sample buffer for 5 min, and subjected to Western blot analysis. For glutathione *S*-transferase (GST) pull-down assays, GST alone or the indicated GST-p73α fusion proteins were expressed in *E. coli* strain DH5α and loaded onto glutathione-Sepharose 4B beads (Amersham Biosciences). PKA-Cβ was generated *in vitro* in the presence of [$^{35}$S]methionine using the TnT quick-coupled *in vitro* transcription/translation system (Promega Corp., Madison, WI) according to the manufacturer's instructions. $^{35}$S-Labeled PKA-Cβ was incubated with GST or GST-p73α fusion proteins bound to glutathione-Sepharose beads for 2 h at 4 °C in a total volume of 400 μl of binding buffer (50 mM Tris-Cl (pH 7.5), 150 mM NaCl, and 0.1% Nonidet P-40). Beads were washed extensively with the same buffer, and the radiolabeled proteins were eluted by boiling in SDS sample buffer for 5 min. Following electrophoresis, gels were destained, dried, and exposed to an x-ray film with an intensifying screen at −80 °C.

*Cell Fractionation*—Transfected COS-7 cells were fractionated into nuclear and cytoplasmic fractions as described previously (30). In brief, cells were washed twice with ice-cold 1× PBS and lysed in lysis buffer B containing 10 mM Tris-Cl (pH 7.5), 1 mM EDTA, 0.5% Nonidet P-40, and protease inhibitor mixture for 30 min at 4 °C. Cell lysates were centrifuged at 15,000 rpm for 10 min at 4 °C to separate soluble (cytoplasmic) from insoluble (nuclear) fractions. The pellets were washed extensively with lysis buffer B and further dissolved in 1× SDS sample buffer. The nuclear and cytoplasmic fractions were analyzed by immunoblotting with anti-lamin B monoclonal antibody (Ab-1, Oncogene Research Products) or with anti-α-tubulin monoclonal antibody (Ab-2, NeoMarkers, Inc.).

*Immunofluorescence Microscopy*—H1299 cells were grown on coverslips and transiently cotransfected with the expression plasmids for hemagglutinin (HA)-p73α and FLAG-PKA-Cβ. Forty-eight hours after transfection, cells were fixed with 3.7% formaldehyde in PBS for 30 min at room temperature and permeabilized with 0.2% Triton X-100 for 5 min. Nonspecific binding sites were blocked by treating cells with PBS containing 3% bovine serum albumin. The cells were incubated with anti-HA polyclonal and anti-FLAG monoclonal antibodies for 1 h, followed by incubation with fluorescein isothiocyanate- and rhodamine-conjugated secondary antibodies (Invitrogen). The coverslips were washed with PBS, mounted onto slides, and observed under a Fluoview laser scanning confocal microscope (Olympus, Tokyo, Japan).

*Luciferase Reporter Assay*—p53-deficient H1299 cells ($5 \times 10^4$ cells in a 12-well plate) were transiently cotransfected with a constant amount of the indicated expression plasmid (HA-p73α, HA-p73β, or p53), a p53/p73-responsive luciferase reporter construct ($p21^{WAF1}$ or *bax*), and pRL-TK encoding *Renilla* luciferase with or without increasing amounts of the expression plasmid for FLAG-PKA-Cβ. The total amount of DNA was kept constant (510 ng) with pcDNA3 per transfection. Forty-eight hours after transfection, cells were lysed and assayed for luciferase activity using the Dual-Luciferase reporter assay system (Promega Corp.) according to the manufacturer's recommendations. The transfection efficiency was normalized based on pRL-TK reporter activity.

*Reverse Transcription-PCR*—H1299 cells were transiently cotransfected with the indicated combinations of expression plasmids. Twenty-four hours after transfection, total RNA was prepared using an RNeasy mini kit (Qiagen Inc.) according to the manufacturer's protocol. One microgram of total RNA was used to synthesize the first-strand cDNA using random primers and SuperScript II reverse transcriptase (Invitrogen). Reverse transcription was carried out at 42 °C for 90 min, and reverse transcripts were amplified by standard PCR with *rTaq* DNA polymerase (Takara, Ohtsu, Japan). The primers used for PCR were as follows: $p21^{WAF1}$, 5′-ATGAAATTCACCCCCTTTCC-3′ (sense) and 5′-CCCTAGGCTGTGCTCACTTC-3′ (antisense); and glyceraldehyde-3-phosphate dehydrogenase, 5′-ACCTGACCTGCCGTCTAGAA-3′

[1] The abbreviations used are: PKA-C, protein kinase A catalytic subunit; PBS, phosphate-buffered saline; GFP, green fluorescence protein; GST, glutathione *S*-transferase; HA, hemagglutinin; ChIP, chromatin immunoprecipitation; $Bt_2$cAMP, dibutyryl cAMP.

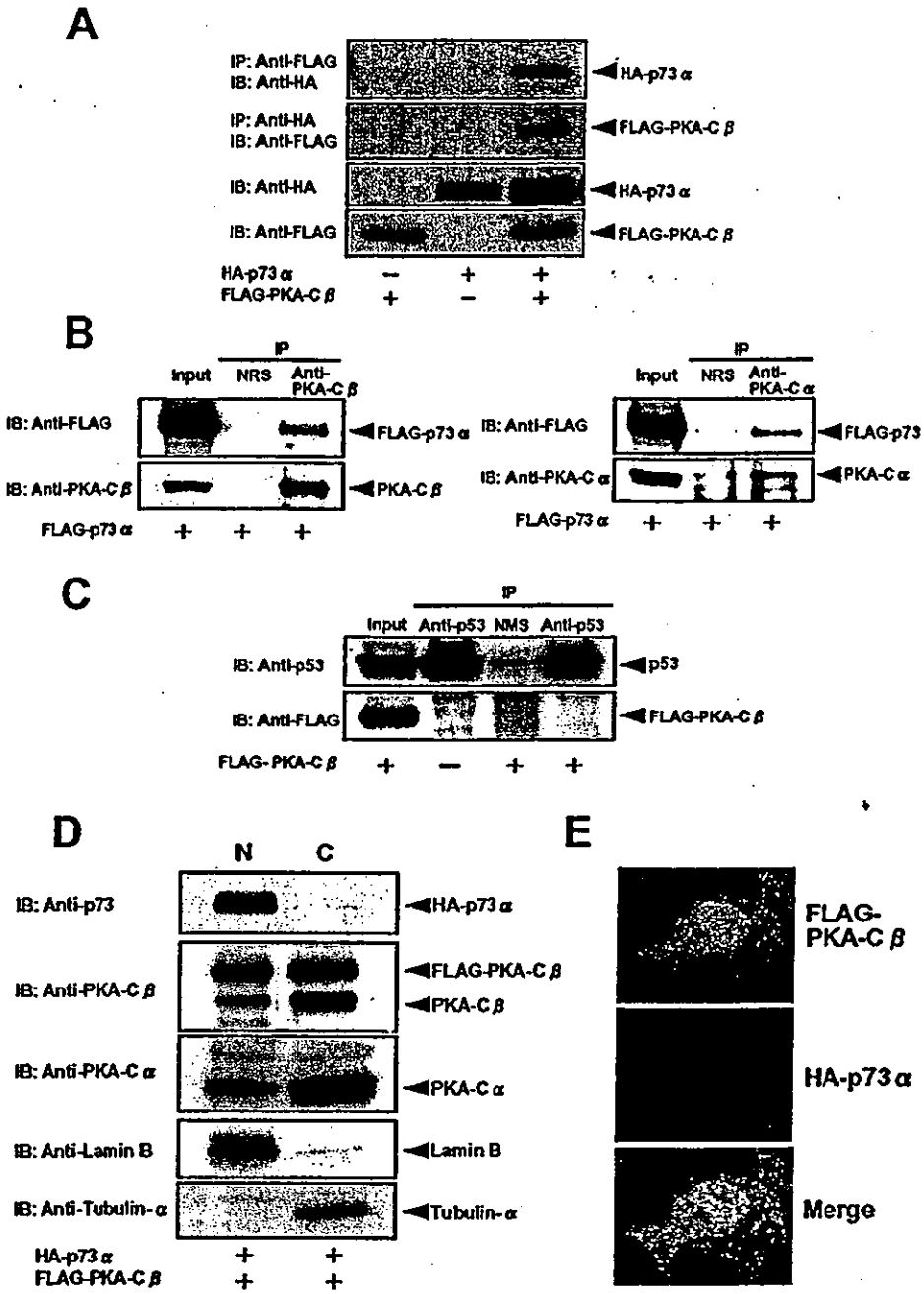


FIG. 1. **Interaction between p73 and PKA-Cβ in mammalian cultured cells.** *A*, p73α forms a complex with PKA-Cβ in COS-7 cells. Whole cell lysates prepared from COS-7 cells transiently cotransfected with the indicated combinations of expression plasmids were immunoprecipitated (*IP*) with anti-FLAG or anti-HA monoclonal antibody. Immunoprecipitates were analyzed by immunoblotting (*IB*) with anti-HA (*first panel*) or anti-FLAG (*second panel*) monoclonal antibody. Whole cell lysates were immunoblotted with anti-HA (*third panel*) or anti-FLAG (*fourth panel*) monoclonal antibody to show the expression of HA-p73α or FLAG-PKA-Cβ, respectively. *B*, p73α binds to endogenous PKA-C in COS-7 cells. COS-7 cells were transiently transfected with the expression plasmid for FLAG-p73α. Forty-eight hours after transfection, whole cell lysates were prepared and subjected to immunoprecipitation with anti-PKA-Cβ (*left panels*) or anti-PKA-Cα (*right panels*) polyclonal antibody. Immunoprecipitation with normal rabbit serum (*NRS*) was used as a negative control. After immunoprecipitation, coprecipitating FLAG-p73α was detected by immunoblotting with anti-FLAG monoclonal antibody. *C*, PKA-Cβ does not bind to endogenous p53. COS-7 cells were transiently transfected with the empty control plasmid or with the expression plasmid encoding FLAG-PKA-Cβ. Forty-eight hours post-transfection, whole cell lysates were prepared and subjected to immunoprecipitation with anti-p53 monoclonal antibody or normal mouse serum (*NMS*), followed by immunoblotting with anti-p53 (*upper panel*) or anti-FLAG (*lower panel*) monoclonal antibody. *D*, subcellular localization of exogenous and endogenous PKA-Cβ. p53-deficient H1299 cells were transiently cotransfected with the expression plasmids for HA-p73α and FLAG-PKA-Cβ (*first* through *third panels*). Forty-eight hours after transfection, transfected cells were fractionated into nuclear (*N*) and cytoplasmic (*C*) fractions as described under "Experimental Procedures." Each fraction was adjusted to an equal volume, and the aliquots of these fractions were separated by 10% SDS-PAGE, followed by immunoblotting with the indicated antibodies. These fractions were analyzed for lamin B (*fourth panel*) and α-tubulin (*fifth panel*) to show the validity of our fractionation technique. *E*, nuclear co-localization of p73 and PKA-Cβ. H1299 cells plated on coverslips were cotransfected with the expression plasmids for HA-p73α and FLAG-PKA-Cβ and processed for immunocytochemical detection using anti-HA and anti-FLAG antibodies. The merged image shows the nuclear co-localization of p73α and PKA-Cβ.

(sense) and 5′-TCCACCACCCTGTTGCTGTA-3′ (antisense). PCR products were separated by 1.5% agarose gel electrophoresis and stained with ethidium bromide.

*In Vitro Kinase Assays*—GST or the indicated GST-p73α fusion proteins bound to glutathione-Sepharose beads were washed three times with kinase buffer (20 mM Tris-Cl (pH 7.5), 100 mM NaCl, and 12 mM $MgCl_2$). The washed beads were incubated with 30 μl of kinase buffer containing 2 units of purified PKA catalytic subunit (Sigma), 2 mM